Technical Report

414

J. Rheinstein

Backscatter From Spheres: A Short Pulse View

27 April 1966

Lincoln Laboratory

MASSACHUSETTS INSTITUTE OF TECHNOLOGY

Lexington, Massachusetts

Distribution of this document is unlimited.

MASSACHUSETTS INSTITUTE OF TECHNOLOGY

LINCOLN LABORATORY

BACKSCATTER FROM SPHERES: A SHORT PULSE VIEW

J. RHEINSTEIN

Group 22

LEXINGTON   MASSACHUSETTS

ABSTRACT

The backscatter from conducting and dielectric spheres, and to a lesser extent from conducting spheres with a relatively thin dielectric coating, is considered in the time domain. Utilizing rigorously computed values of the amplitude and phase of the continuous wave backscatter, short pulses of electromagnetic waves are synthesized by Fourier series. The resultant returns are examined as a function of time, and the individual returns compared with some approximate theories.

CONTENTS

BACKSCATTER FROM SPHERES: A SHORT PULSE VIEW

I. INTRODUCTION

The problem of the scattering of electromagnetic waves from a sphere has received considerable attention due to a large extent to the fact that the rigorous solution has been known for a long time.* The rigorous solution, known as the Mie series, allows numerical results to be obtained to a high degree of accuracy. It has, however, various drawbacks which have led to the development of numerous approximate or asymptotic solutions. Probably the main failing of the rigorous solution is that it does not readily allow construction of a physical model of the phenomena involved. Such a model would be useful for studying the scattering from spheres with parameters different from those for which computations are available, and could lead to an under-standing of electromagnetic scattering from other than spherical shapes. In addition, the con-vergence of the series is relatively slow,† so that even with the utilization of high speed digital computers the cases which have been considered are limited.

The various approximate techniques — which include geometrical optics,[4] the Fresnel-Kirchhoff theory of diffraction,[4] Keller's geometrical theory of diffraction,[5,6] creeping wave theory,[7,8] and Fock theory[9,10] — are not limited to the sphere. A study of the sphere, however, provides a good check of these theories and models and often indicates how they may be modified or com-bined to handle the specific case under consideration.[11,12] Backscatter from a conducting sphere now appears to be well understood[13] and, as will be shown, the application of physical optics and creeping wave theory leads to results in good agreement with the rigorous solution. Such is not the case, however, with the dielectric sphere, where the approximate techniques often have only limited success.

Generally any comparison between the rigorous results and the various models which have been developed is carried out in the frequency domain; in this report the scattering from con-ducting, dielectric, and, to a lesser extent, from dielectric coated conducting spheres, is ex-amined in the time domain. A consideration of the time domain has achieved considerable suc-cess in many areas and, as will be shown, appears to lead to an improved understanding of the scattering from spheres. Utilizing the Mie series, values for the amplitude and phase of the scattered electric field for continuous waves are computed. By means of Fourier series, the response, as a function of time, to an incident impulse or pulse comparable in extent to the size of the sphere (short pulse) is synthesized. In this report, however, only the short pulse response will be considered.

---

* See Logan[1] for a fascinating account of the history of this problem. Reference 2 lists much of the recent work.

† Generally the number of terms required is slightly greater than 1.2ka, where $k = 2\pi/\lambda$ and a is the sphere radius.[3]

The resultant scattering from most objects may generally be considered to be due to various components; however, in the frequency domain it is often difficult to separate or distinguish these. Different components have often traveled different optical paths and are then distinguishable in the time domain. The dispersion of the components is generally small enough so that appreciable spreading of the pulse does not occur. By these methods the presence of the various components is vividly illustrated and further insight into the scattering is obtained. For conducting spheres, for example, the validity of the decomposition into optics and creeping wave components is demonstrated and it is shown that this decomposition is valid to quite large wavelengths. It will also be shown that some of the returns, of an appreciable magnitude, from dielectric spheres, which have generally not been considered previously, appear to have the character of creeping waves.

The scattering of short pulses, or impulses, of electromagnetic waves by means of Fourier (or Laplace) transforms has been considered previously by Kennaugh and his co-workers.[14-20] Their primary aim was to approximate the impulse response for targets that were not spherical, thereby obtaining an estimate of the CW scattering. A limited number of theoretical studies and some experimental results have also been reported in the literature.[21-30]

II. SHORT PULSE SYNTHESIS

The plane polarized electric field incident upon the scatterer is taken to be

$$E^i(t) = \begin{cases} e(t) \cos \omega_c t & -\tau \leqslant t \leqslant \tau \\ \\ 0 & \tau < |t| < T \end{cases} \tag{1}$$

where 2τ is the incident pulse length, ω_c is the carrier angular frequency, and, in this report, the envelope $e(t)$ is

$$e(t) = 0.5 \left[1 + \cos(\pi t/\tau)\right] \quad . \tag{2}$$

A pulse train of period $2T$ is obtained by expanding Eq. (1) in a Fourier series

$$E^i(t) = \frac{a_o}{2} + \sum_{m=1}^{\infty} a_m \cos(m\omega_o t) \tag{3}$$

where

$$\omega_o = \frac{\pi}{T} \quad .$$

In Eq. (3) use is made of the fact that $E^i(t)$, as given by Eqs. (1) and (2), is an even function. The coefficient a_m of each term in Eq. (3) is the weighting coefficient of the corresponding frequency $m\omega_o$ in the spectrum of $E^i(t)$, determined by the values of ω_c, τ and T desired. These coefficients may be found by standard Fourier techniques.[31]

The (complex) electric field scattered at a large distance by a target is then given by

$$E^s(t) = K \sum_{m=1}^{\infty} A(m\omega_o) e^{i\varphi(m\omega_o)} a_m \cos(m\omega_o t) \tag{4}$$

2

where $A(m\omega_o)$ and $\varphi(m\omega_o)$ are the amplitude[*] and phase of the CW scattered electric field at the angular frequency $m\omega_o$ and K is a constant, depending on the range to the target. Equation (4) was programmed for a digital computer to calculate $E^S(t)$ when $A(m\omega_o)$, $\varphi(m\omega_o)$, τ, ω_c, and T were input.

Plotting the real, or imaginary, part of (4) as a function of time presents a picture of the instantaneous electric field as a function of time. Plotting the modulus of (4) presents the envelope of the scattered electric field. In this report time is measured in terms of the free space transmit time of a sphere radius.

For the results presented in this report the required amplitudes and phases were numerically computed on a digital computer by the Mie series. The accuracy of the short pulse calculations is determined by the increment in a/λ at which the rigorous calculations are carried out, the point at which the series in Eq. (4) is truncated, and the accuracy of the Mie series calculations. It is necessary that the increment in the calculations be small enough to give a reasonably smooth representation of the CW backscatter cross section as a function of a/λ. For the purposes of this report the Mie series calculations were carried out for increments of 0.01 in a/λ. Plots of the CW backscatter cross section were made to give an indication of the effect of this sampling. Except for the case of dielectric coated conducting spheres, it is believed that this increment is small enough to give a reasonably accurate representation of the short pulse response. In fact the reason for choosing an increment this small was primarily to obtain a reasonably large value of T in order to obtain a relatively large unambiguous (nonaliased or "nonfolded-over") response in the time domain. An increment of 0.01 in a/λ implies an unambiguous range of 50 sphere radii. Generally 800 terms were retained in the series given by Eq. (4). This is usually sufficient to give reasonable results for the present purpose for pulse widths of one sphere radius or larger and for values of the carrier wavelength λ_c less than or equal to four sphere radii.

The programs utilized for the Mie series calculations are modifications of the program described in Ref. 3. The most critical part of the calculation is the evaluation of the required Bessel and Neumann functions. The program contains built in checking procedures, which are independent of the calculation algorithms to insure that sufficient accuracy in these functions as well as in other parts of the calculation is retained to give at least five significant figures in the result. The programs have also been extensively compared with hand calculations as well as various published data.[†]

---

[*] The convention employed here relates the amplitude and phase to the backscatter cross section $\sigma(m\omega_o)$ by

$$\frac{\sigma(m\omega_o)}{\pi a^2} = \left| A(m\omega_a) e^{i\varphi(m\omega_o)} \right|^2 \,.$$

The phase angle $\varphi(m\omega_o)$ is as defined on page 286 of Van de Hulst,[4] except that the phase reference is shifted a distance τ in front of the sphere.

† Of the literature checked the only serious discrepancy noted was in the calculations for a complex index of refraction given in Ref. 32. A considerable number of digital computer as well as hand calculations, utilizing different algorithms, have led to the conclusion that the published data are in error. In some cases the error is as much as a factor of two.

TABLE I

POSITION OF THE MAXIMA AND MINIMA OF THE NORMALIZED BACKSCATTER FROM A CONDUCTING SPHERE

Position of Maxima (a/λ)	Differences	Cross Section $(\sigma/\pi a^2)$	Position of Minima (a/λ)	Differences	Cross Section $(\sigma/\pi a^2)$
0.1636		3.65495	0.2775		0.285041
	0.1981			0.1932	
0.3717		1.96958	0.4707		0.505600
	0.1942			0.1919	
0.5659		1.58864	0.6626		0.634592
	0.1919			0.1917	
0.7578		1.41048	0.8543		0.716232
	0.1917			0.1915	
0.9495		1.30698	1.0458		0.772456
	0.1918			0.1916	
1.1413		1.24023	1.2374		0.813423
	0.1918			0.1918	
1.3331		1.19398	1.4292		0.844286
	0.1918			0.1916	
1.5249		1.16016	1.6210		0.868137
	0.1920			0.1920	
1.7169		1.13451	1.8130		0.887011
	0.1920			0.1921	
1.9089		1.11453	2.0051		0.902239
	0.1922			0.1922	
2.1011		1.09864	2.1973		0.914714
	0.1922			0.1923	
2.2933		1.08576	2.3896		0.925057
	0.1924				
2.4857		1.07515			

III. SCATTERING FROM A CONDUCTING SPHERE

The well-known plot of the backscatter cross section of a conducting sphere as a function of a/λ, where a is the sphere radius and λ the wavelength, is presented in Fig. 1. The data for this figure, as well as the associated phases, were numerically computed utilizing the Mie series.[33] While this rigorous method provides accurate results it does not lead to an understanding of the physical phenomena which lead, for example, to the damped oscillations, or ripples, evident in Fig. 1. The general methods of physical optics or geometrical optics also do not predict or explain these ripples.
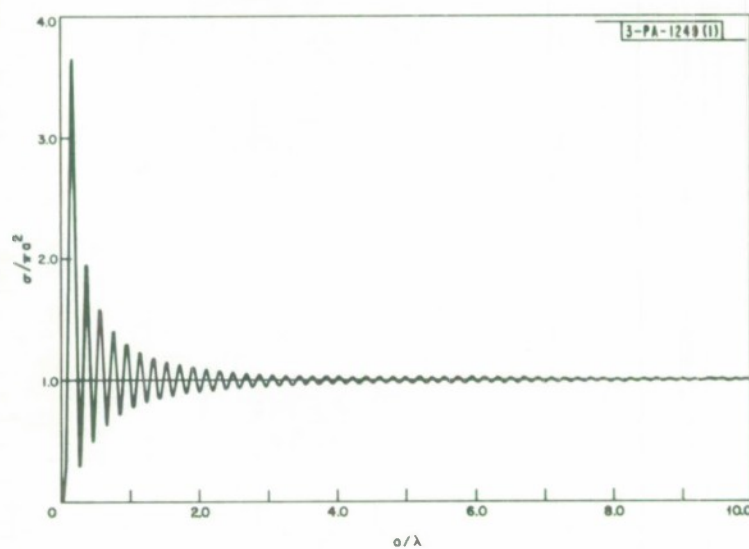

Fig. 1. Backscatter cross section of conducting sphere (computational increment 0.01 or smaller in a/λ).

The regularity of these ripples, as indicated by Table 1, leads one to suspect that two returns may exist which, through interference, combine to give the calculated curve. According to Logan,[1] Franz, upon seeing a curve such as Fig. 1, suggested that the ripples could be explained by assuming that there was interference between waves reflected at the front, specular portion of the sphere and waves which, by traveling around the rear portion of the sphere as shown in Fig. 2, had traveled a distance $(2 + \pi)a$ further. From this model, with no modifications, one would expect the maxima, or minima, to be spaced at intervals of $0.194a/\lambda$. Franz,[7,8] and his co-workers, continued working on the problem and developed the now well-known creeping wave analysis of the scattering from spheres and cylinders, although generally they considered only the scalar problem. Senior and Goodrich[13] have given the vector solution to the problem. Such waves are also inherent in the work of Fock[10] and of Keller.[6]

In such a creeping wave analysis the rigorous Mie series is generally converted into a contour integral by means of a modified Watson transformation. The resultant integral may then, in turn, be separated into two contour integrals. One of these, known as the optics integral, may be evaluated by a saddle-point technique and gives terms whose phase closely corresponds to scattering from the specular portion of the sphere. For backscatter the first terms in this asymptotic series are*

---

* See Logan[34] (as of this date Vol. III of the report referenced in [34] has not been issued). See also Senior and Goodrich.[13]
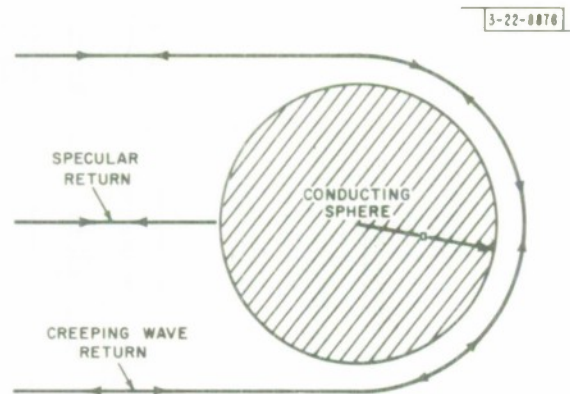
Fig. 2.   Diagram of specular and creeping wave returns.
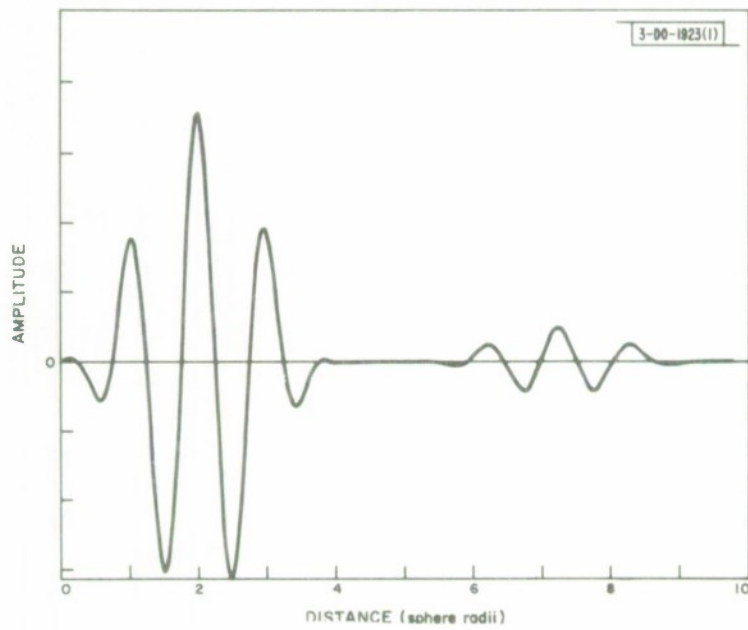

Fig. 3.   Short pulse response of conducting sphere ($\tau = 2o$, $T = 25a$, $o/\lambda_c = 1$).

$$A_o e^{i\varphi_o} = \left[1 - \frac{i}{2ka} + \frac{1}{2(ka)^4} + \ldots \right] e^{-2ika*}$$

(5)

where

$$k = \frac{2\pi}{\lambda}\ .$$

The first term in this series is that predicted by geometrical optics, and simple physical optics gives the first two terms.

The second contour integral, known as the creeping wave integral, may be evaluated as a sum of residues of poles. The phase of these terms corresponds to waves which have circumnavigated the shadow region of the sphere making $N + \frac{1}{2}$, $N = 0, 1, 2, \ldots$ revolutions around the sphere. Equations suitable for the calculation of the amplitude and phase of these returns are given by Senior and Goodrich.[13]

Both the optics and the creeping wave returns are evident in the results of calculations of the scattering of short pulses from conducting spheres as shown in Figs. 3 through 7. In Figs. 4 through 7 the amplitude A, corresponding to the peak of the envelope of each return, is given above the return, and the position of the peak of the return is presented on the bottom scale of each figure. The amplitude of the first return agrees closely with that predicted by physical or geometrical optics for the specular return ($A^2 = \sigma/\pi a^2 \approx 1.0$). The peak of the second return occurs just slightly further than $(2 + \pi)a$ behind the first return, corresponding to the increase in the path length traveled. The slight excess in delay is attributed to the fact that the waves may be considered as having phase and group velocities less than the velocity of light in a vacuum, or that these creeping waves may be considered as traveling at a small distance out from the surface of the sphere.[†]

These results, and similar results presented by Kennaugh and Moffatt[16-19] indicate that the separation of the backscatter from conducting spheres into optics and creeping wave terms is not just convenient mathematically, but that these waves may, in some sense, be considered to exist physically.

Creeping wave returns have also been observed experimentally on static radar ranges with high resolution. Foreman and Sedivec[26] and Alongi, Kell and Newton[27] have reported observing the creeping wave return from conducting cone spheres. Figure 8 presents the results of some short pulse measurements carried out on conducting spheres,[‡] which also show the specular and the creeping wave returns. Two of the figures, 8(b) and 8(j), show the return from a flat plate (half-dollar), and Fig. 8(a) shows the background return, for comparison. The pulse length employed for these measurements, approximately four nanoseconds, is relatively long in comparison with the transit time of the diameters of the spheres measured. Thus, because of interference effects, the two returns are not as distinctly seen as in the results of the calculations presented in Figs. 3 through 7. The presence of the two returns is, however, quite apparent.

The results presented thus far, while illustrating the presence of two returns in the backscatter from a conducting sphere, do not lend themselves readily to a quantitative comparison with the results of theoretical creeping wave analysis. In order to conduct such a comparison

---

* The units ore such thot $\sigma/\pi o^2 = A^2$.

† See Van de Hulst,[4] p. 368.

‡ These measurements were corried out on the short pulse rodor ronge of Generol Dynamics (Fort Worth, Texas), and were obtained with the help of Mr. D. F. Sedivec of M. I. T. Lincoln Loborotary.

Fig. 4. Envelope of short pulse response of conducting sphere ($\tau = 1a$, $T = 25a$, $a/\lambda_c = 1$).

Fig. 5. Envelope of short pulse response of conducting sphere ($\tau = 1a$, $T = 25a$, $a/\lambda_c = 2$).
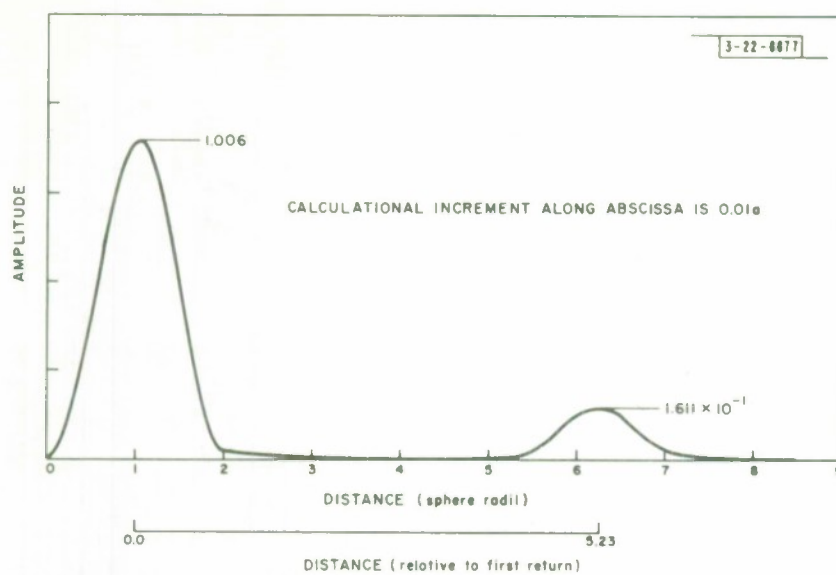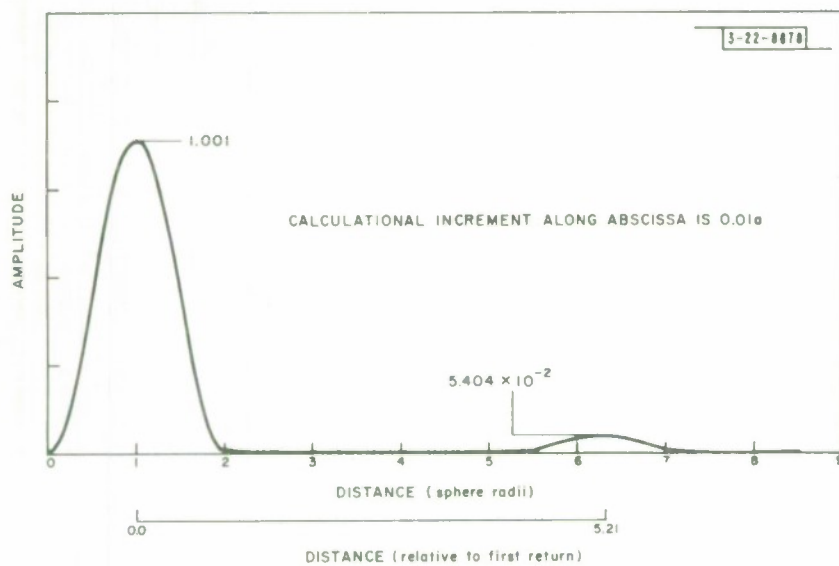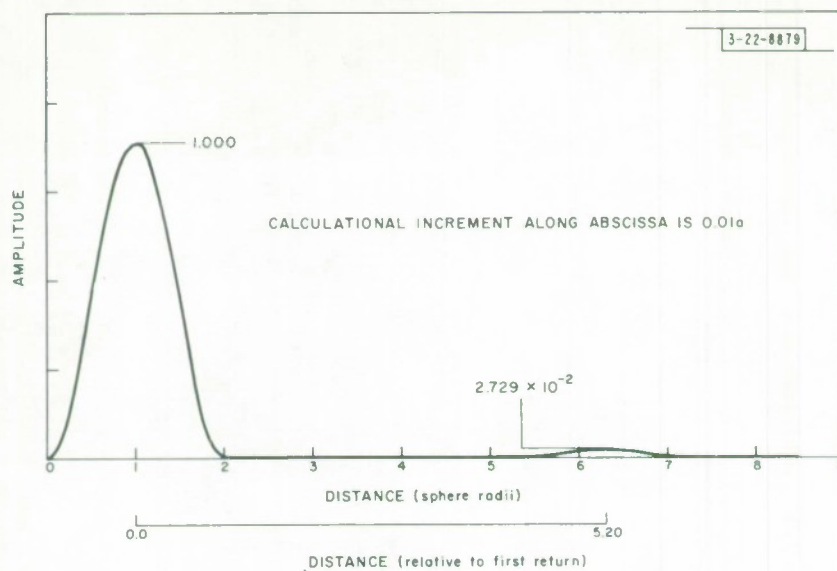
Fig. 6. Envelope of short pulse response of conducting sphere ($\tau = 1a$, $T = 25a$, $a/\lambda_c = 3$).
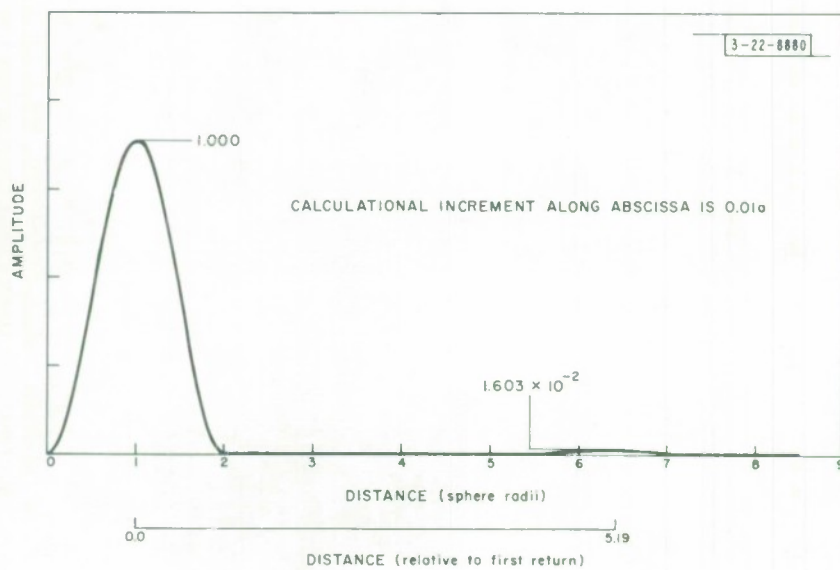
Fig. 7. Envelope of short pulse response of conducting sphere ($\tau = 1a$, $T = 25a$, $a/\lambda_c = 4$).
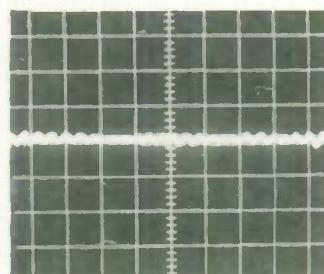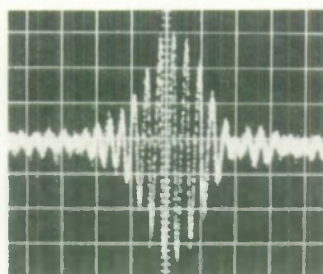
TARGET	MOUNT	HALF DOLLAR	2.5-in.* SPHERE
ATTENUATION (db)	20	20	20
	(a)	(b)	(c)
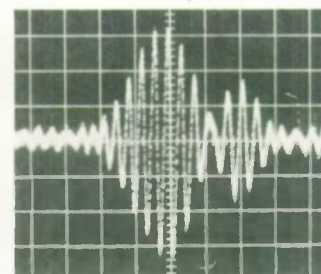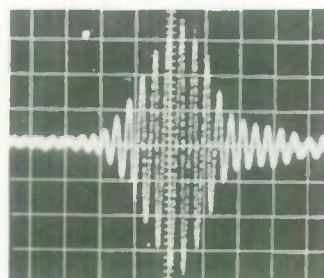
TARGET	3.0-in. SPHERE	4.0-in. SPHERE	4.5-in. SPHERE
ATTENUATION (db)	26	28	28
	(d)	(e)	(f)
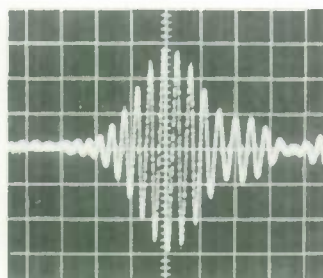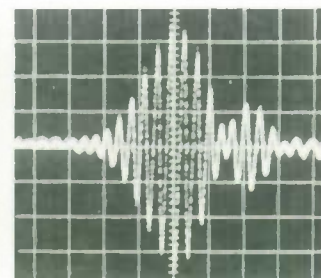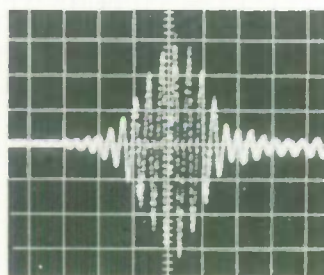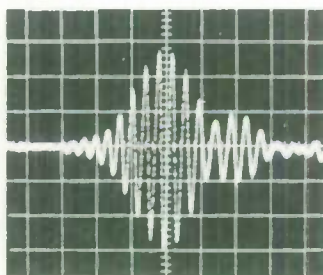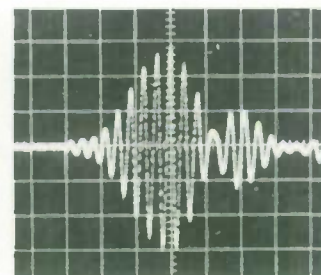
TARGET	5.0-in. SPHERE	6.0-in. SPHERE	7.7-in. SPHERE
ATTENUATION (db)	32	32	34
	(g)	(h)	(i)
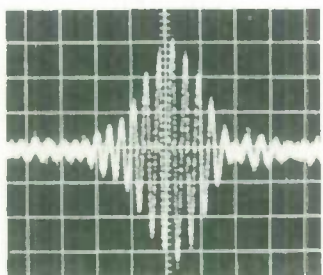
TARGET
ATTENUATION (db)

HALF DOLLAR
20
(j)

* DIAMETER

-30-9535-1

Fig. 8(a-j).   Results of experimental measurements of short pulse scattering of some conducting spheres.

10

and to obtain a somewhat different view of the phenomena, each return, the specular and the creeping wave, was separately transformed back to the frequency domain. The short pulse response in the time domain was split into two parts, one of which was nonzero during the extent of the specular return and the other nonzero only during the extent of the creeping wave return. These two parts were then separately Fourier analyzed, and the resulting Fourier coefficients, corresponding to a frequency $m\omega_o$, were divided by the corresponding Fourier coefficients a_m [see Eqs. (3) and (4)] originally employed in the short pulse syntheses. The results obtained are presented in Figs. 9 through 11. These calculations were carried out utilizing double precision arithmetic on the case $\tau = a$, $\lambda_c = a$. Because of various errors inherent in the computation, the magnitude of the computed results corresponding to the smaller values of a/λ (up to $a/\lambda \sim 0.05$) are probably somewhat in error, although it is believed that the shape of the curve is roughly correct. Various computations, as well as a consideration of the fact that the computed specular and creeping wave returns should combine to give the return obtained by the Mie series, lead to the estimate that the error is no more than a factor of two.

Figure 9 shows the cross section (normalized to πa^2) for the specular return obtained from the short pulse calculations as compared with that predicted by the first two, or three, terms of Eq. (5). One of the more interesting features of this comparison is the rather close agreement between the computed frequency response and that given by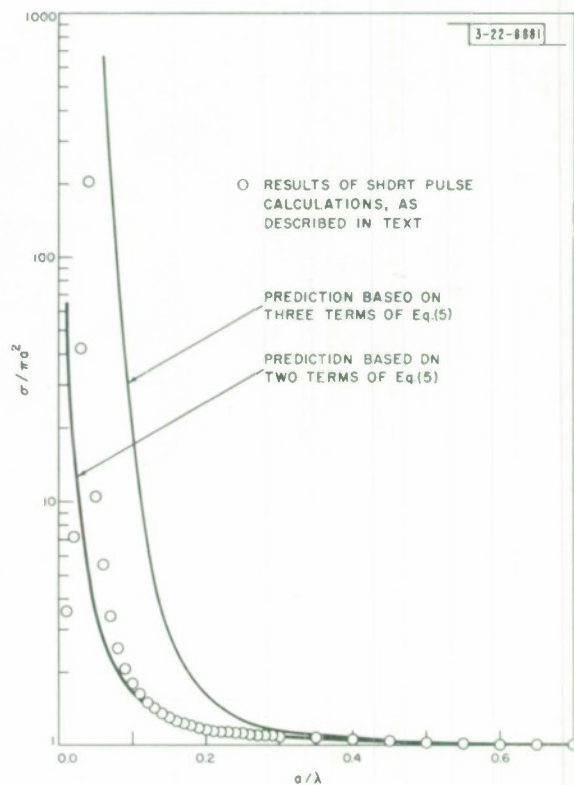 the first two terms of Eq. (5) for values of a/λ approaching 0.1. As Senior[12] points out, the agreement is good even when the sphere presents an area which is less than the first Fresnel zone ($a/\lambda = 0.25$). Figure 10 presents a similar comparison between the creeping wave returns as calculated from the short pulse response, and those given by Eq. (32) of Senior and Goodrich.[13] Five terms in each sum of this equation were retained. Again the comparison is relatively good for a/λ as small as 0.1 or so.

Fig. 9. Comparison of cross section of specular return as found from short pulse response and as predicted by Eq. (5).

O RESULTS OF SHORT PULSE CALCULATIONS, AS DESCRIBED IN TEXT

PREDICTION BASED ON THREE TERMS OF Eq.(5)
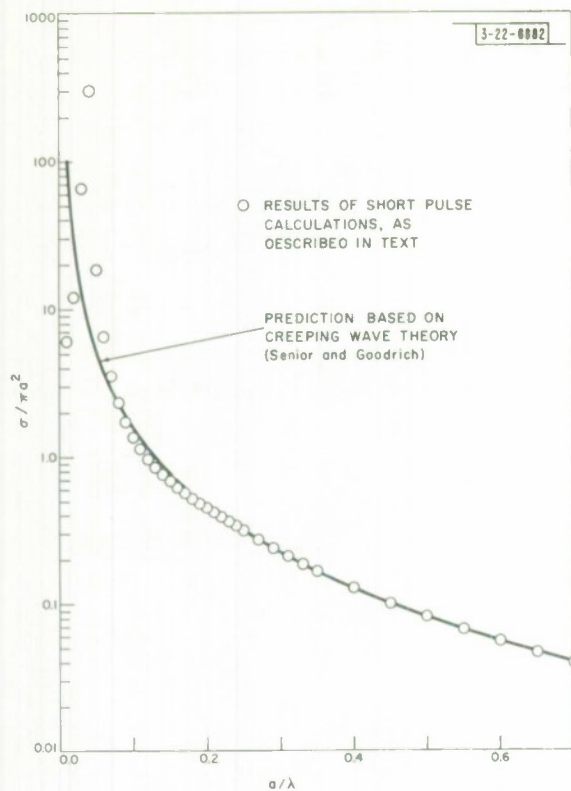
PREDICTION BASED ON TWO TERMS OF Eq.(5)

Fig. 10. Comparison of cross section of first creeping wave return as found from short pulse response and as predicted by creeping wave theory.
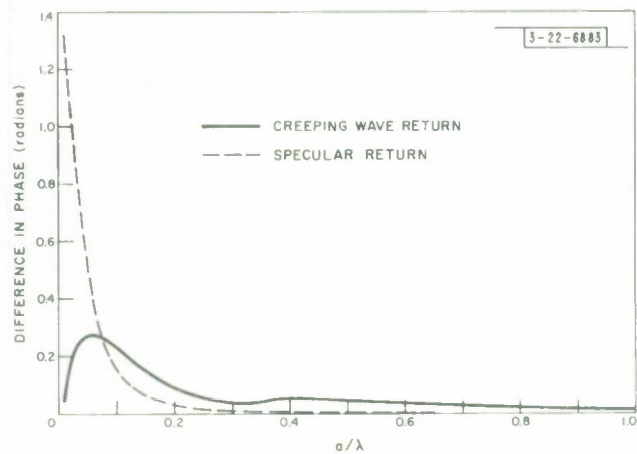

Fig. 11. Difference between phase predicted and that found from short pulse response.

A comparison between the phase of the return as computed from the short pulse response and the approximate theories is presented in Fig. 11. The figure shows the difference between the phase, in radians, as calculated from the short pulse response, and as predicted by the first two terms of Eq. (5) for the specular return and Eq. (32) of Senior and Goodrich for the creeping wave return.

A consideration of these results should give considerable confidence to the results of creeping wave theory, and to the use of these results in studying the scattering from conducting bodies with other than spherical shapes.[17,35,36]

IV. SOLID DIELECTRIC SPHERES

A. Introduction

The use of the synthetic short pulse in analyzing the backscatter from a solid dielectric sphere brings to light many interesting features. Because of the penetrability of such a sphere many different ray bundles, from the geometrical optics point of view, are possible, and interferences between these bundles lead to relatively complicated relationships between the backscatter cross section and the radius of the sphere. A typical plot of the cross section vs a/λ for a lossless sphere is shown in Fig. 12. Several attempts have been made to find approximate means for predicting the scattering from dielectric spheres,* and in some instances good results have been obtained for a range of a/λ. It will be shown that, at least in some cases, such attempts have failed to take into account all of the contributions of an appreciable magnitude. Even though not all of the returns evident in the short pulse response of a dielectric sphere have been identified and explained, most of the returns of an appreciable magnitude will be discussed and a tentative identification given.

B. Prediction of the Position of Returns

Relatively simple ray tracing considerations suffice to predict the position of at least a portion of the contributions to the backscatter from a dielectric sphere observed in the short pulse response. In this section such returns will be described briefly, and the optical path lengths for each predicted return presented. A more complete discussion may be found in the literature.[4,37-43] A different type of return, not predicted by these techniques will also be discussed.

As in the case of the conducting sphere a specular return due to paraxial rays reflected from the front surface of the sphere is expected. This is known as the front axial return and is labeled 1 in Fig. 13. The optical paths of all other returns will be referenced to this front axial return.

A second return is expected from a ray bundle (labeled 2 in Fig. 13) which also propagates along the axis. This return, known as the rear axial return, is transmitted at the first boundary, reflected at the rear boundary, and again transmitted at the front boundary. It is expected to appear a distance P behind the front axial return where

$$P = 4ma \qquad (6)$$

is the optical path length.[†] m is the (real part of the) index of refraction.

---

* A description of such work is given by Peters, et al.;[37] see also Chap. 12 of Von de Hulst,[4] and Refs. 38-43.

† The phase of the return, usually presented in the literature, is determined not only by the optical path but also by any phase shifts arising either from reflections or from the presence of caustics. As pointed out by Dr. S. L. Borison, these phase shifts do not affect the position of the return and cannot generally be observed in the plots presented of the envelope of the short pulse response. Such phase shifts may be observed on plots of the instantaneous electric field as a function of time, but will not be considered further here. See, for example, Von de Hulst,[4] Chap. 12.

COMPUTATIONAL INCREMENT IS 0.01 IN a/λ
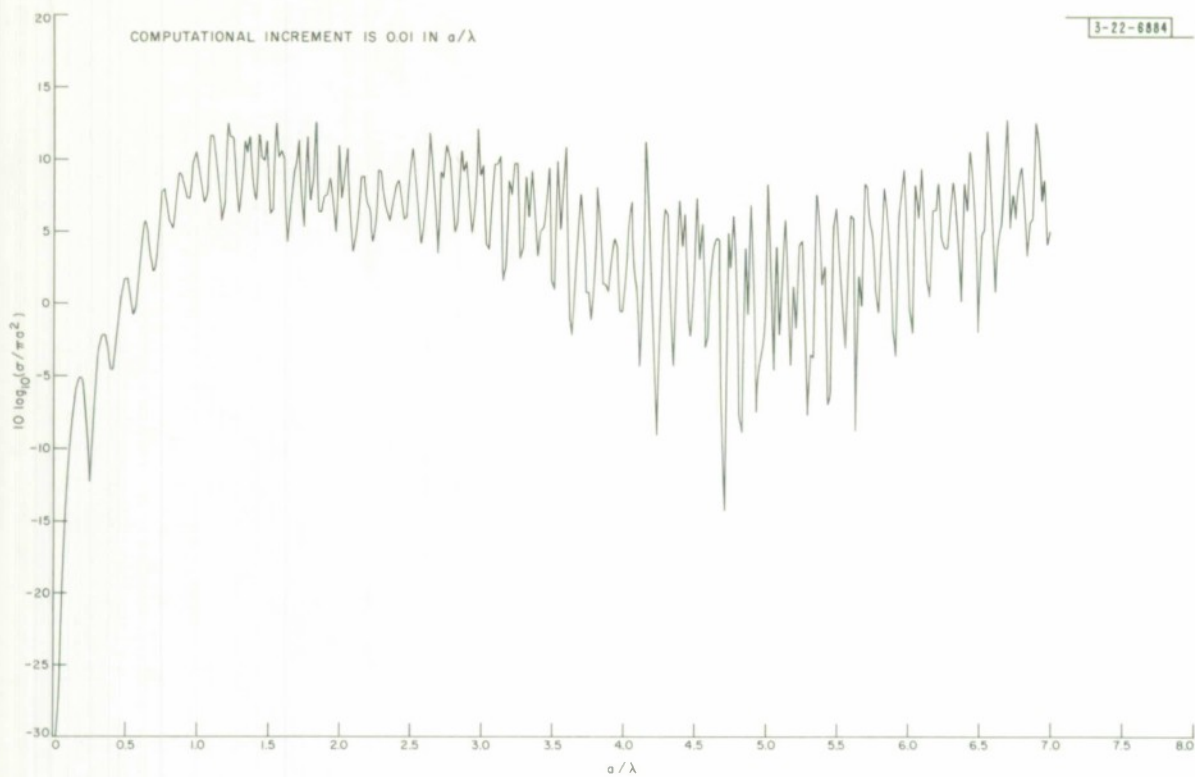
Fig. 12. Backscatter cross section of lossless dielectric with m = 1.6.

SPHERE

1: FRONT AXIAL RAY
2: REAR AXIAL RAY
3: GLORY RAY
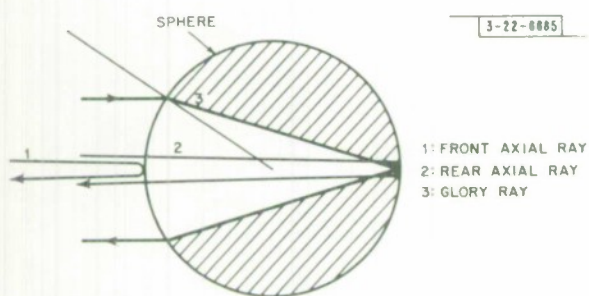
Fig. 13. Diagram showing several possible scattered ray bundles from dielectric sphere.
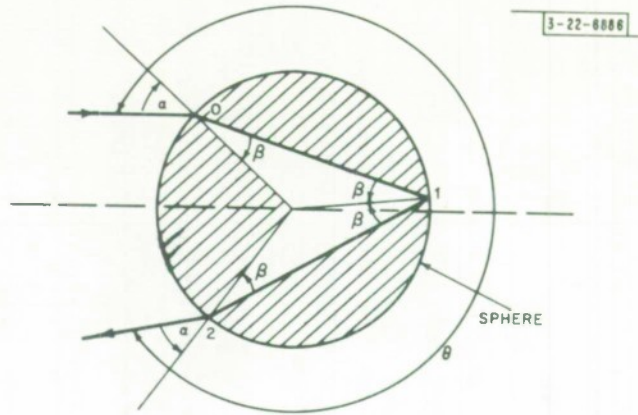
Fig. 14. Geometry employed in prediction of returns.

While the front and rear axial returns, and additional axial returns which have undergone $2r + 1$, $r = 1, 2, 3, \ldots$, internal reflections, are expected from any dielectric sphere, there exists a set of nonaxial returns whose presence or absence depends upon the index of refraction. Such a return, for example, is the glory ray, labeled 3 in Fig. 13. Referring to Fig. 14 a ray incident at 0 parallel to the axis is refracted at the surface of the sphere, the ray is reflected at 1, and then again refracted out of the sphere at 2. In general, the angle Θ shown in Fig. 14 is given by

$$\Theta = 2\alpha + p(180° - 2\beta) \tag{7}$$

where $p - 1$ internal reflections have taken place, and the angles α and β are related by Snell's law

$$\sin \alpha = m \sin \beta \quad ; \quad 0° \leqslant \alpha, \ \beta \leqslant 90° \quad . \tag{8}$$

If $\Theta = 360°N$, $N = 1, 2, 3, \ldots$, then the ray will leave the sphere parallel to the axis and contribute to the backscatter. The optical path length for such rays, found from the geometry, is

$$P = 2 \left[mp \cos \beta + (1 - \cos \alpha) \right] a \quad . \tag{9}$$

$2mpa \cos \beta$ is the optical path Q traversed in the sphere, and the distance $2a(1 - \cos\alpha)$ is traversed in free space.

For given values of p and N,[*] simultaneous solutions for real values of α and β may be found for only certain ranges of values of m, indicating that the corresponding rays exist only for these m. For the single bounce glory ray (ray 3 in Fig. 13), $p = 2$ and $N = 1$, so that from Eq. (7), with $\Theta = 360°$, it is found that $\alpha = 2\beta$. From Eq. (8)

$$m \sin\beta = \sin\alpha = \sin 2\beta = 2 \sin\beta \cos\beta$$

so that

$$\frac{m}{2} = \cos\beta \quad .$$

---

* The geometry of the problem, as well as the forms of Eqs. (7) and (8) requires that $p \geqslant 2N$.

15

		TABLE II				
		PARAMETERS OF PREDICTED BOUNCE RAYS, m = 1.6				
N	p	α (degrees)	β (degrees)	Optical Path (sphere radii)	ϵ_1^2	ϵ_2^2
1	2	73.75	36.87	6.56	1×10^{-1}	7×10^{-2}
2	5	47.75	27.55	14.8	2×10^{-4}	7×10^{-9}
3	7	27.55	16.79	21.7	1×10^{-7}	2×10^{-9}
3	8	50.45	28.80	23.2	8×10^{-7}	2×10^{-16}
4	9	19.75	12.19	28.2	2×10^{-10}	2×10^{-11}
4	10	36.10	21.61	30.1	3×10^{-10}	6×10^{-15}
4	11	51.35	29.21	31.5	3×10^{-9}	4×10^{-24}
4	12	69.30	35.78	32.4	2×10^{-6}	3×10^{-17}
5	11	15.45	9.59	34.9	4×10^{-13}	6×10^{-14}
5	12	28.55	17.38	36.8	3×10^{-3}	1×10^{-16}
5	13	40.35	23.87	38.5	7×10^{-13}	5×10^{-21}
6	14	23.70	14.55	43.5	4×10^{-16}	1×10^{-18}
6	15	33.60	20.24	45.4	5×10^{-16}	5×10^{-22}
6	16	42.90	25.18	46.9	2×10^{-15}	2×10^{-28}
6	17	52.10	29.53	48.1	5×10^{-14}	$< 10^{-30}$
6	18	61.85	33.43	49.1	7×10^{-12}	$< 10^{-30}$
6	19	74.80	37.09	50.0	4×10^{-7}	4×10^{-19}
7	15	10.75	6.72	47.5	2×10^{-18}	6×10^{-19}
7	16	20.30	12.52	50.1	7×10^{-19}	5×10^{-21}
7	17	28.90	17.58	52.1	6×10^{-19}	8×10^{-24}
7	18	36.90	20.05	53.8	1×10^{-18}	8×10^{-28}

Since $\cos \beta \leqslant 1$ we find $m \leqslant 2$. Also, since

$$\alpha = 2\beta \leqslant 90°$$

$$\beta \leqslant 45°$$

$$\frac{m}{2} \geqslant \cos 45° = \frac{\sqrt{2}}{2}$$

thus,

$$m \geqslant \sqrt{2} \quad .$$

Thus for a ray with $p = 2$, $N = 1$, the index of refraction must lie in the interval $\sqrt{2}$ to 2. Similar reasoning leads to the result that for $p = 3$, $N = 1$,[*] m must lie in the range 0 to $2/\sqrt{3}$.

In order to determine which rays could exist for the cases to be discussed below ($m = 1.6$ and 2.5), Eqs. (7) and (8) were programmed for, and solved on, a digital computer. The results for all ray bundles whose optical path is less than 50 sphere radii are presented in Tables II and III, where α[†] and β are the angles defined in Fig. 14, the optical path is computed from Eq. (9), and ϵ_1^2 and ϵ_2^2[‡] are the power reflection coefficients. The divergence which will be mentioned later is not included.

According to Peters,[37] stationary rays which also contribute to the backscatter, are possible and should be considered. That is, a bundle of rays for which, from Eq. (7)

$$\frac{d\Theta}{d\alpha} = 0 \tag{10}$$

and Θ is close to $360°N$, $N = 1, 2, 3, \ldots$, or $\Theta' = \Theta(\mathrm{mod}\ 360°) \approx 0°$, may also contribute to the backscatter. Equations (7), (8) and (10) imply that

$$\frac{\sin \alpha}{\sin \beta} = p \frac{\cos \alpha}{\cos \beta} = m \quad . \tag{11}$$

This equation was programmed for a digital computer, and the results for $m = 1.6$ and 2.5 are listed in Tables IV and V.

The ray bundles listed in Tables II through V are those which previously have received primary consideration when approximate models for the backscatter from dielectric spheres have been developed. It will be shown later that, at least for the cases considered, these ray bundles do not account for all of the returns observed and some of these unaccounted returns have appreciable amplitude. One possible explanation for these returns is presented below.

In his discussion of the observed ripples of the computed extinction[§] curve for various dielectric spheres, Van de Hulst[¶] observes that the present theories, based on ray tracing, do not appear to explain the periodicity of these ripples. He then puts forward a tentative explanation based on surface waves. Because some of the returns observed in the short pulse analysis appear to fit well with this idea, and do not appear to agree with standard ray tracing results, a short discussion is presented below.

---

* This ray bundle is sometimes also called a glory ray.

† The angle α is presented to the closest 0.05 degree.

‡ The subscript 1 refers to parallel or E-plane polarization and the subscript 2 refers to perpendicular or H-plane polarization.

§ The extinction of a body as defined by Van de Hulst[4] (p. 3) is a measure of the total energy removed from the incident beam by scattering as well as by absorption.

¶ Reference 4, p. 375.

N	p	a (degrees)	β (degrees)	Optical Path (sphere radii)	ϵ_1^2	ϵ_2^2
				TABLE III		
		PARAMETERS OF PREDICTED BOUNCE RAYS, m = 2.5				
4	9	38.85	14.20	44.0	1×10^{-5}	3×10^{-8}
5	11	27.65	10.70	54.2	1×10^{-7}	4×10^{-9}
5	12	58.00	19.83	57.4	2×10^{-5}	1×10^{-17}
6	13	22.00	8.61	64.4	4×10^{-9}	2×10^{-10}

TABLE III

PARAMETERS OF PREDICTED BOUNCE RAYS, m = 2.5

TABLE IV

PARAMETERS OF PREDICTED STATIONARY RAYS, m = 1.6

p	a (degrees)	β (degrees)	Optical Path (sphere radii)	θ (degrees)	θ' (degrees)
2	43.90	25.68	6.17	345.07	−14.93
3	63.79	34.11		462.94	102.94
4	71.20	36.27		572.20	−147.80
5	75.25	37.19	13.66	678.64	−41.36
6	77.80	37.65		783.76	63.76
7	79.60	37.93		888.15	168.15
8	80.95	38.11		992.09	−87.91
9	81.95	38.23	24.61	1095.73	15.73
10	82.80	38.32		1199.17	119.17
11	83.45	38.38		1302.47	−137.53
12	84.05	38.43	31.33	1405.65	−34.35
13	84.45	38.46		1508.75	68.75
14	84.85	38.50		1611.78	171.78
15	85.20	38.52		1714.76	−85.24
16	85.50	38.54	42.20	1817.69	17.69
17	85.80	38.56		1920.59	120.59
18	86.00	38.57		2023.46	−136.54
19	86.20	38.58	48.85	2126.31	−33.69
20	86.40	39.59		2229.13	69.13

			TABLE V		
		PARAMETERS OF PREDICTED STATIONARY RAYS, m = 2.5			
p	o (degrees)	β (degrees)	Optical Poth (sphere radii)	θ (degrees)	θ' (degrees)
3	35.90	13.56		530.41	170.41
4	53.75	18.82	19.36	676.95	−43.05
5	62.10	20.70		817.18	97.18
6	67.20	21.64		954.74	−125.26
7	70.70	22.18	33.94	1090.88	10.88
8	73.20	22.52		1226.16	146.16
9	75.15	22.75	42.25	1360.88	−79.12
10	76.70	22.91	48.50	1495.22	55.22
11	77.95	23.03		1627.28	−172.72
12	78.95	23.12	56.25	1763.13	−36.87
13	79.80	23.18		1896.83	96.83
14	80.55	23.24		2030.40	−129.60
15	81.20	23.28	70.65	2163.87	3.87

From geometrical optics it is well-known that if a ray passes from a dense to a rare medium, the angle of incidence α being smaller than the critical angle of total internal reflection α_c, some of the energy will be transmitted to the rarer medium, and some will be reflected as shown in Fig. 15(a). If, however, α is greater than α_c then total internal reflection will take place as shown in Fig. 15(b). If the angle of incidence α is equal to the critical angle α_c [see Fig. 15(c)] then some energy will be refracted with $\beta = 90°$, i.e., this energy will travel along the surface as a type of surface wave.[*] After traveling along the surface some distance, part of the energy may again enter the denser medium.

In Fig. 16 a ray strikes the sphere at grazing incidence and begins to circumnavigate the sphere. At the point A, for example, it may enter the sphere at the critical angle, leaving again at the point B. A similar situation may occur at A' and B' and, indeed, along the entire path of the ray. The optical path through the sphere is $m \cdot AB$. From Fig. 16

$$\sin \gamma = \sin(90 - \alpha_c) = \cos \alpha_c$$

$$= \frac{1/2 \ AB}{a} \tag{12}$$

and since, from Snell's law

$$m = \frac{1}{\sin \alpha_c}$$

---

* The intensity of this ray bundle is zero occording to the Fresnel formula; however, o more detailed examinotion indicates that it may have an appreciable magnitude. There was a considerable discussion of this type of wave in the Annolen der Physik in the period from 1947 to 1955. See, for example, Refs. 44–49 which include experimental as well as theoretical results.
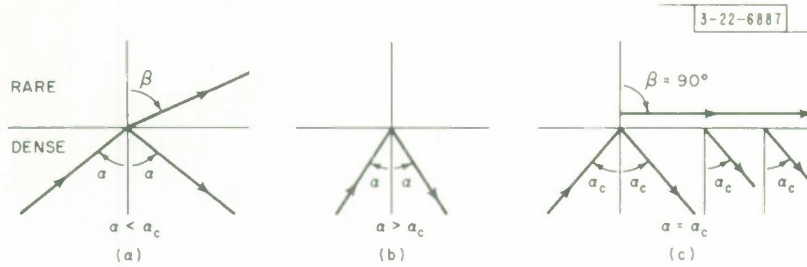
Fig. 15.   Diagram of surface wave obtained when angle of incidence equals critical angle α_c.
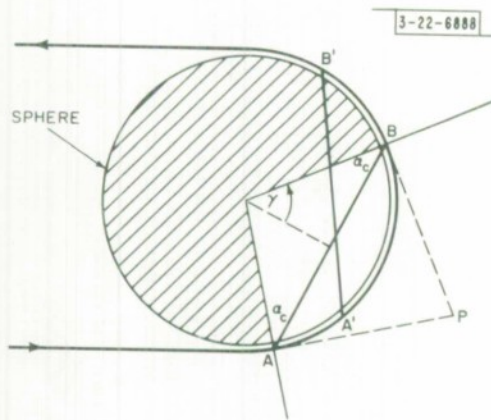
Fig. 16.   Geometry for calculation of optical path of surface wave.

the optical path becomes

$$m \cdot AB = \frac{2a}{\tan \alpha_c} \quad .$$

(13)

Also, from Fig. 16

$$AP = BP = \frac{1/2 \, AB}{\cos (90 - \alpha_c)}$$

$$AP + BP = \frac{AB}{\sin \alpha_c} \quad .$$

From Eq. (12)

$$AB = 2a \cos \alpha_c \quad .$$

Thus

$$AP + BP = \frac{2a}{\tan \alpha_c} = m \cdot AB \quad .$$

(14)

The increase in the optical path due to taking a "short cut" through the sphere rather than staying on the surface is thus

$$ha = \frac{2a}{\tan \alpha_c} - 2a \, \alpha_c \quad .$$

(15)

20

As the wave travels around the sphere it will take M "short cuts," each time increasing the optical path length by the amount ha. The full optical path around the body, and the delay with respect to the front axial return, which might be expected on a plot of the short pulse return, is

$$P = [2 + (2N - 1) \pi + Mh]a \quad . \tag{16}$$

Van de Hulst states that the number of short cuts taken will probably be close to the maximum number possible, M_{max}, which is the largest integer smaller than $(2N - 1) \pi/2\alpha_c$. Such a return appears to have many features in common with the creeping wave return from a conducting sphere described earlier. A return of this type is, in fact, obtained in the creeping wave analysis of a dielectric cylinder reported by Beckmann and Franz.[50] Figure 13 of Reick[51] vividly shows the presence of this type of surface wave for a dielectric cylinder. Tables VI and VII present optical paths, as given by Eq. (16), for the returns expected for m = 1.6 and 2.5, respectively.

C. Short Pulse Analysis

Having summarized the returns which might be expected, we shall proceed to analyze the short pulse response of a dielectric sphere. From the foregoing it is evident that many returns might be expected, some with very long path lengths, or delays, with respect to the first, front axial, return. Because a Fourier series representation is employed in this analysis, returns with long delays will appear "folded over" and it becomes difficult, if not impossible, to identify

TABLE VI		
PARAMETERS OF PREDICTED SURFACE WAVES, m = 1.6		
$\alpha_c = 51.4°$, h = 0.7067		
N	M	Optical Path (sphere radii)
1	1	5.85
	0	5.14
2	5	14.96
	4	14.25
	3	13.54
3	8	23.36
	7	22.65
	6	21.95
4	12	32.47
	11	31.76
	10	30.35
5	15	40.87
	14	40.18
	13	39.46

TABLE VII		
PARAMETERS OF PREDICTED SURFACE WAVES, m = 2.5		
α_c = 66.4°, h = 2.264		
N	M	Optical Path (sphere radii)
1	1	7.41
	0	5.14
2	4	20.48
	3	18.22
	2	15.95
3	6	31.29
	5	29.03
	4	26.76
	3	24.50
4	9	44.37
	8	42.10
	7	39.84
	6	37.58
5	12	57.44
	11	55.18
	10	52.91
	9	50.65
	8	48.39

the returns.[*] For this reason a small absorption coefficient, κ, was employed, i.e., the index of refraction n was taken to be complex

$$n = m + i\kappa \quad .$$

This does not alter the previous analysis to any appreciable extent except that the magnitude of each return is reduced approximately by the factor F

$$F = \exp\left[\frac{-2\pi\kappa}{\lambda_c}\frac{Q}{m}\right][\dagger] \tag{17}$$

where Q is that portion of the optical path P traversed in the sphere itself. This attenuates those returns with the longer path lengths, eliminating most of the "folded over," or aliased, returns. The value of κ utilized was 0.01. Figures 17 and 18 present plots of the normalized backscatter cross section $\sigma/\pi a^2$ vs a/λ for solid dielectric spheres with n = 1.6 + i 0.01 and n = 2.5 + i 0.01, respectively.

Some typical results of the short pulse calculations showing the scattered electric field, at a large distance from the scatterer, from a plane wave incident on a dielectric sphere with n = 2.5 + i 0.01, are presented in Figs. 19 through 23. As before, the position of the principle returns observed in Figs. 20 through 23 relative to the peak of the front axial return, is given on the bottom scale of the figures, and the normalized amplitude A above the curve.[‡] In Table VIII the principal returns observed in Figs. 20 through 23 are identified, primarily on the basis of their position, and compared with the returns predicted in Tables III, V and VII. It may be seen that in general the agreement is good, particularly for those returns having an appreciable magnitude. The presence of the surface waves also appears to be relatively well established. The difference between the observed and predicted positions of these returns may, as in the case of conducting spheres considered earlier, be due to the phase, or group, velocity of these waves being less than the speed of light in vacuum. The identification of the returns attributed to stationary rays is quite tentative.

It is believed that at least a part of those returns which are not identified in Table VIII are "folded over"[§] and actually occur at distances greater than 49.5a from the peak of the front axial return. For example, the unidentified return at 28.25a (a/λ_c = 2.0) may perhaps be identified as the folded-over (P = 70.75a) return of the stationary ray (p = 15) predicted at 70.65a. The question of fold-over could be settled either by employing a larger absorption coefficient or by increasing the distance between ambiguities T. The latter would require the calculation of the amplitude and phase of the CW scattering with increments smaller than 0.01 in a/λ.

The identification of some of the returns is also made difficult by the limited resolution due to choosing τ = 0.5a for this calculation. Increasing the resolution by narrowing the pulse width does not always clear up the picture. As the bandwidth increases other complications arise due primarily to the truncation of the series in Eq. (4) at a/λ = 8, corresponding to 800 terms.

---

[*] This was in fact found to be the case for computations carried out with n = 1.60 + i0.0.

[†] Each term, corresponding to the frequency $n\omega_o$, in the Fourier series is attenuated by the factor $\exp[(-2\pi\kappa/\lambda_n) \times (Q/m)]$. The form given in Eq. (17) should give reasonable results provided the bandwidth is not too large. In particular, wavelengths longer than λ_c are attenuated less and wavelengths shorter than λ_c are attenuated more than given by Eq. (17).

[‡] The units are such that $\sigma/\pi a^2 = A^2$.

[§] A "folded over" return, in the first ambiguity, with a true optical path P will appear on these plots at the position P' = 2T − 2τ − P.

COMPUTATIONAL INCREMENT IS 0.01 IN a/λ
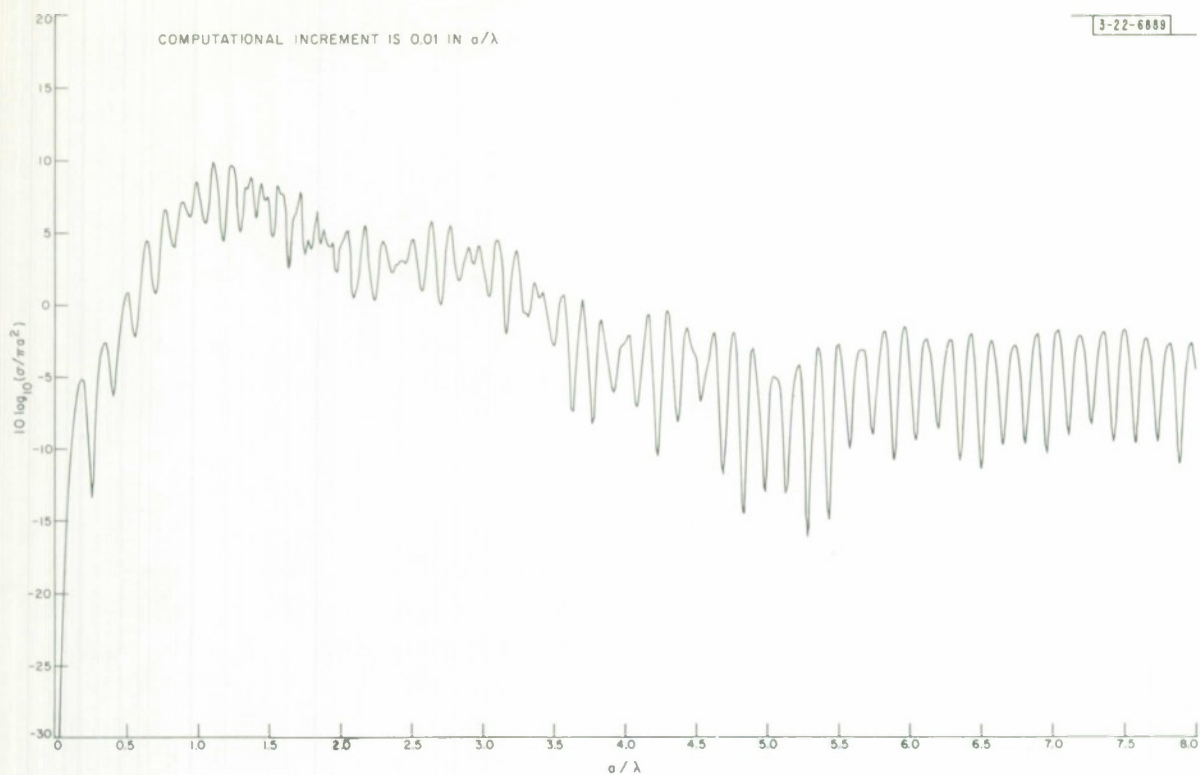
Fig. 17. Backscatter cross section of lossy dielectric sphere with n = 1.6 + i0.01.

COMPUTATIONAL INCREMENT IS 0.01 IN a/λ
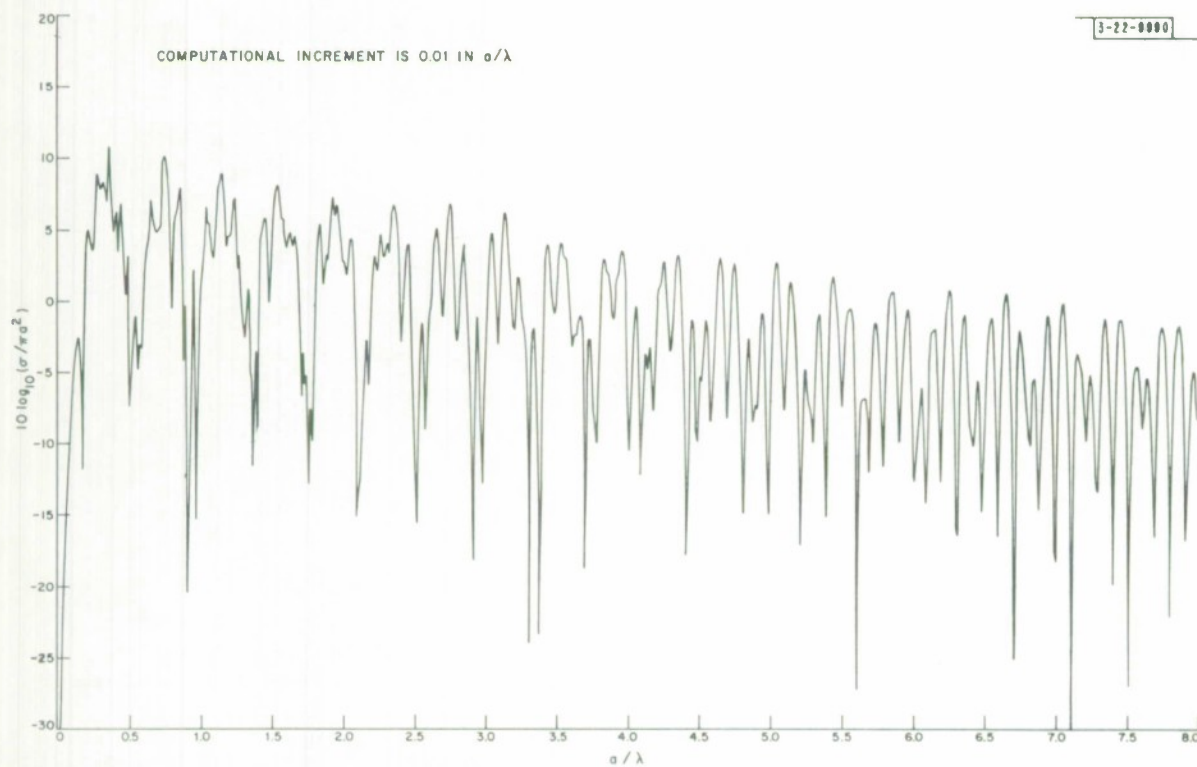
Fig. 18. Backscatter cross section of lossy dielectric sphere with n = 2.5 + i0.01.

Fig. 19. Short pulse response of dielectric sphere, $n = 2.5 + i0.01$ ($\tau = 0.5a$, $T = 50a$, $a/\lambda_c = 4.0$).

Fig. 20. Envelope of short pulse response of dielectric sphere, $n = 2.5 + i0.01$ ($\tau = 0.5o$, $T = 50o$, $a/\lambda_c = 1.0$).

Fig. 21. Envelope of short pulse response of dielectric sphere, $n = 2.5 + i0.01$ ($\tau = 0.5a$, $T = 50a$, $a/\lambda_c = 2.0$).

27

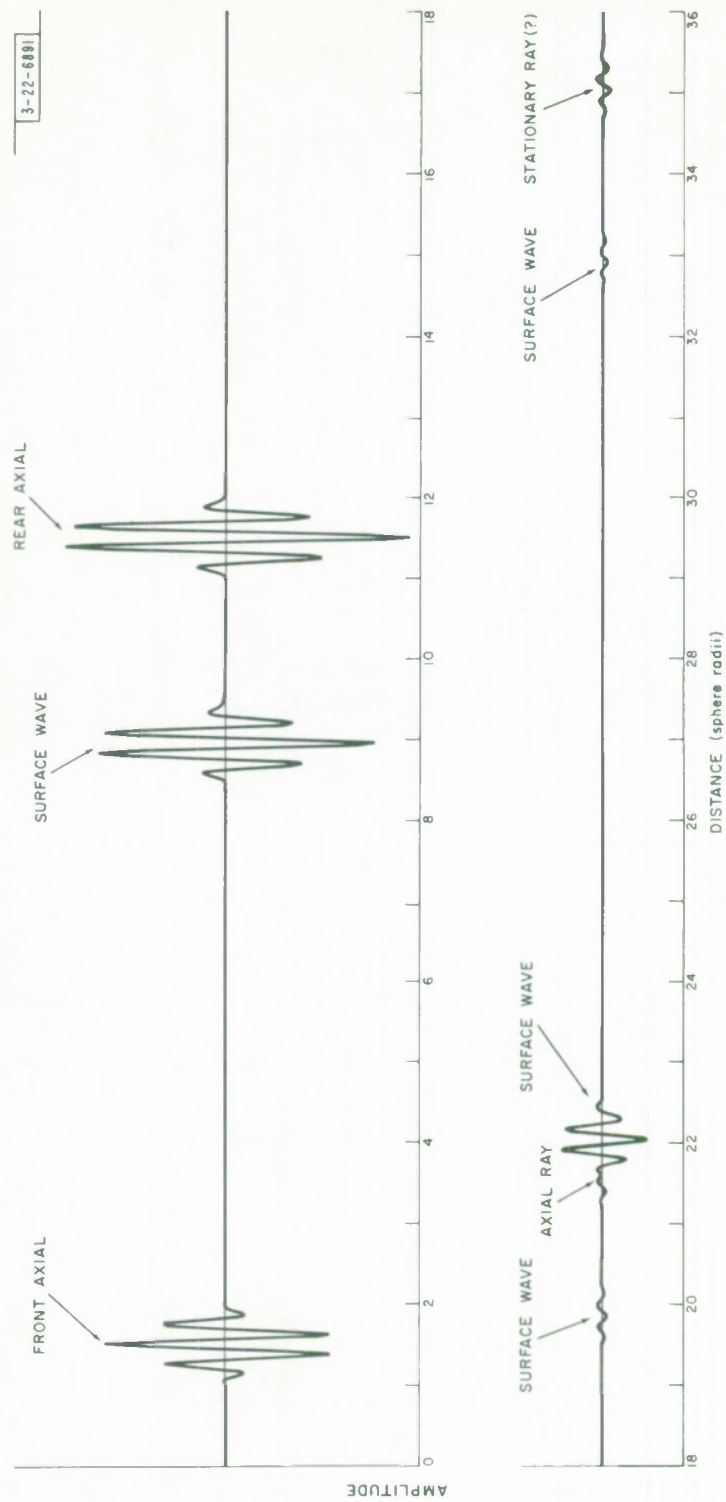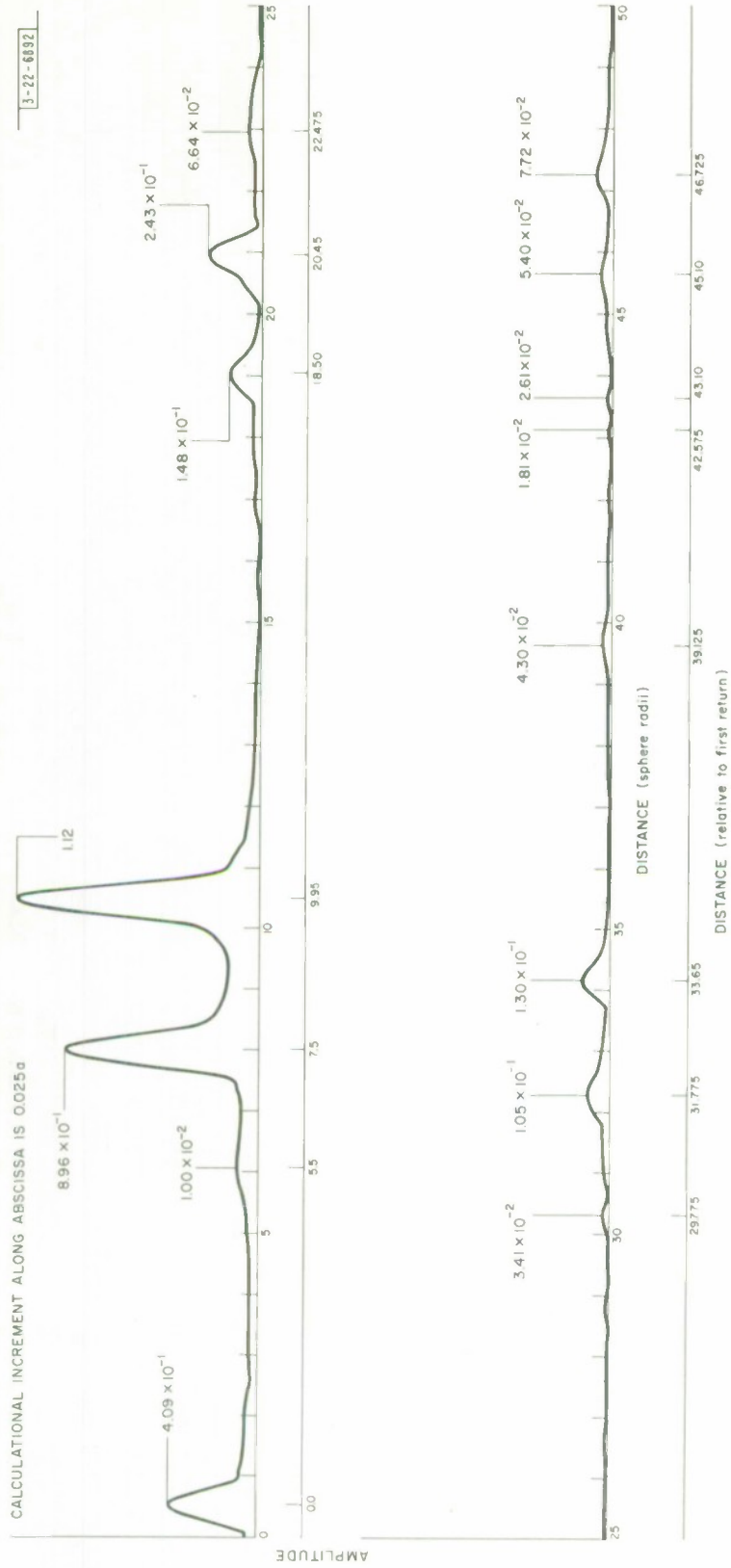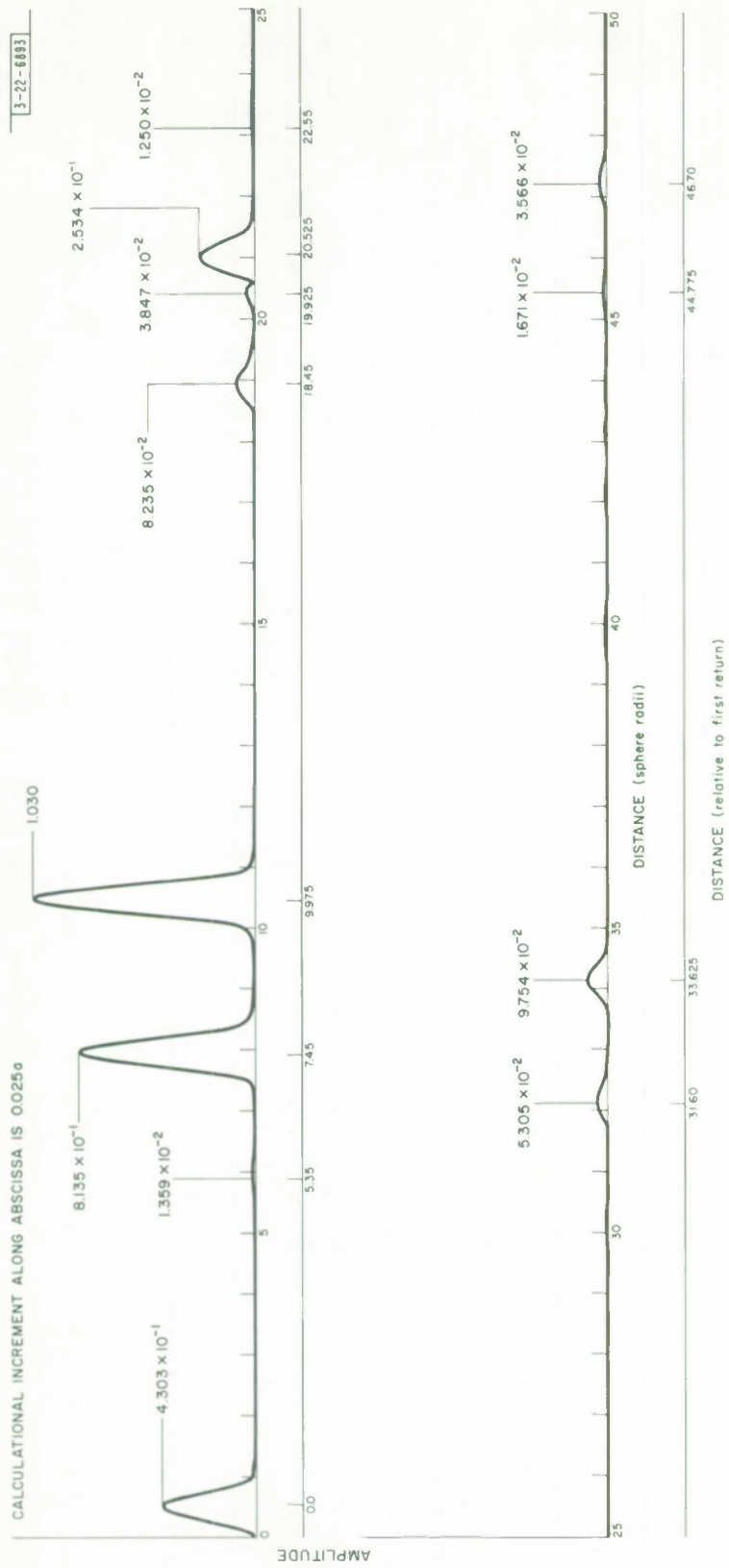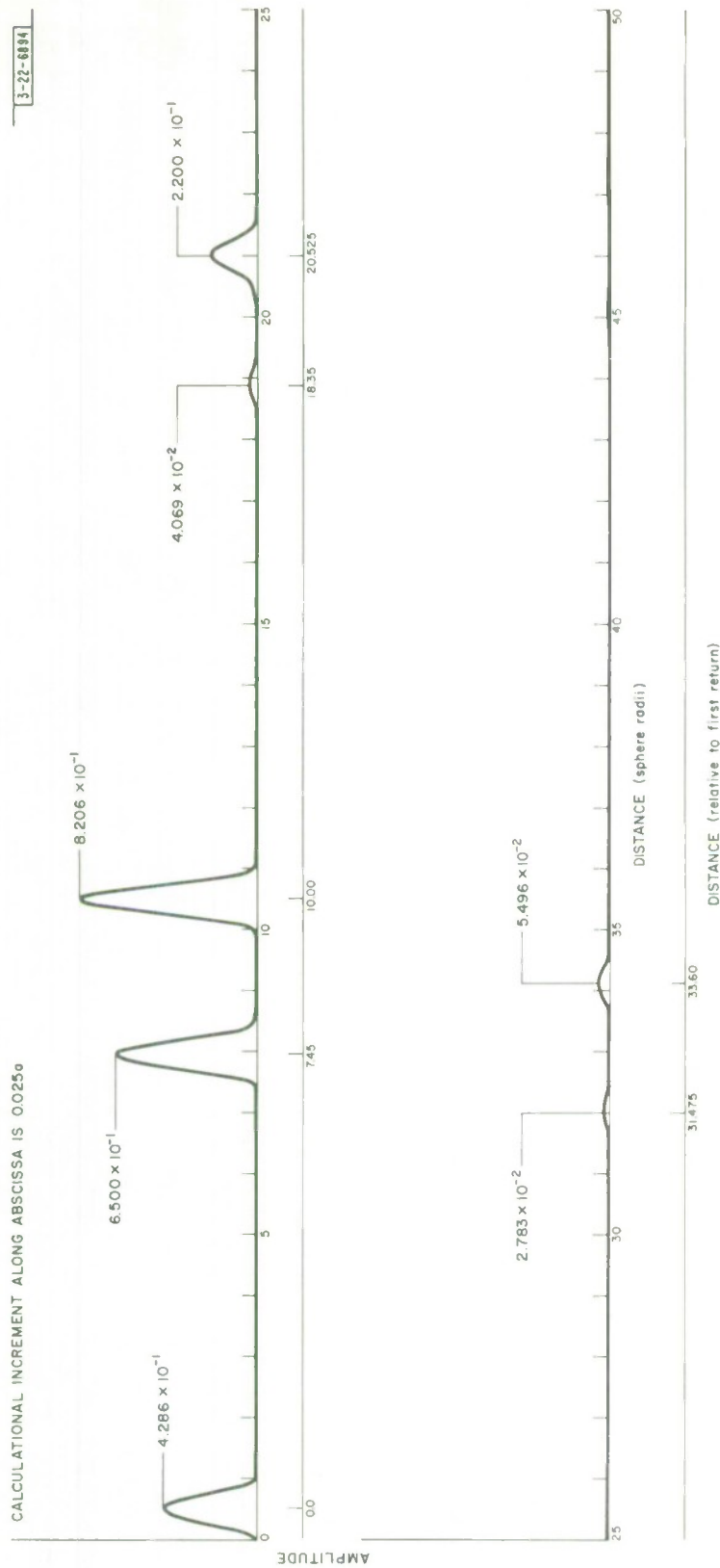Fig. 22. Envelope of short pulse response of dielectric sphere, $n = 2.5 + i0.01$ ($\tau = 0.5a$, $T = 50a$, $a/\Lambda_c = 3.0$).
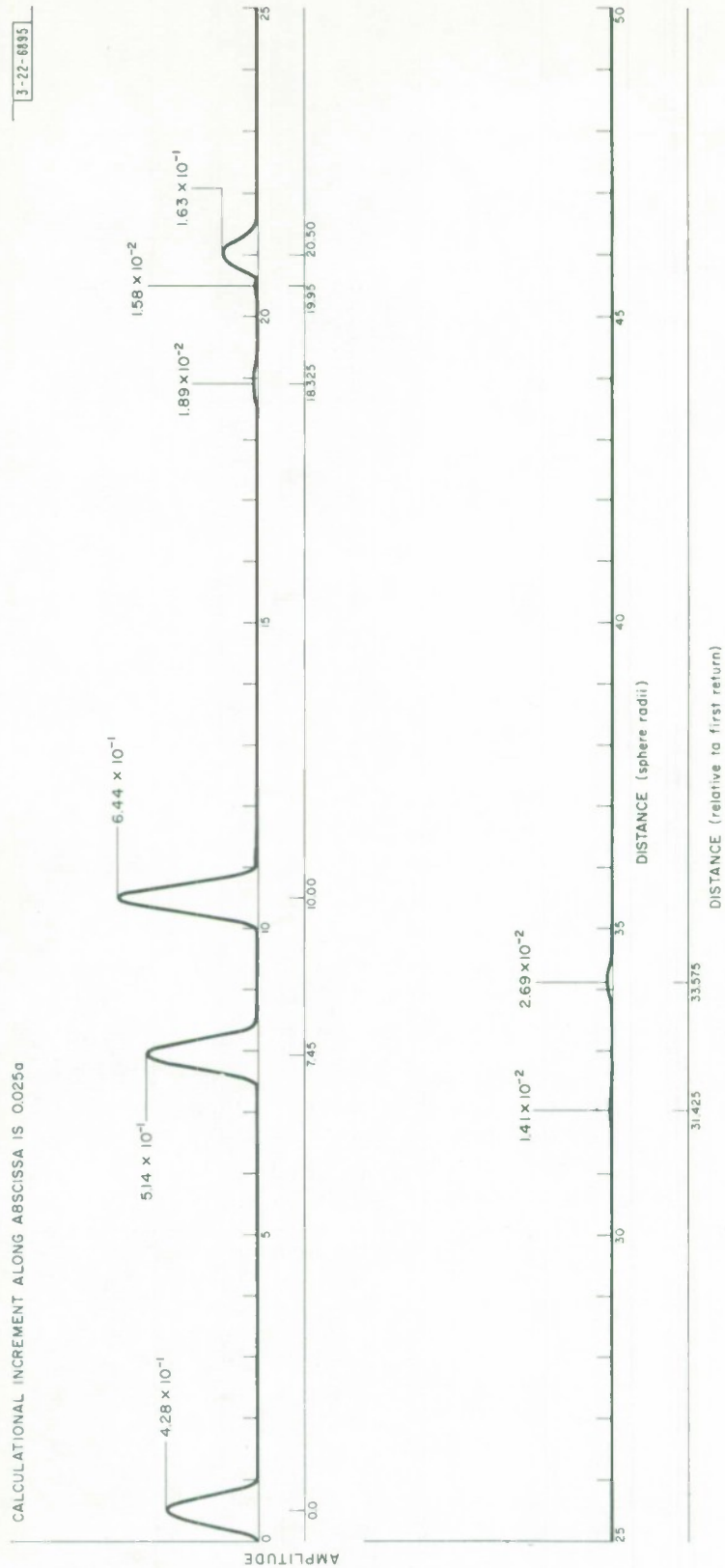
28

Fig. 23. Envelope of short pulse response of dielectric sphere, n = 2.5 + i0.01 ($\tau = 0.5a$, T = 50a, $a/\lambda_c = 4.0$).

TABLE VIII

COMPARISON OF THE POSITION OF THE PREDICTED AND OBSERVED RETURNS, $m = 2.5$

Position of Observed Return (relative to peak of front axial return) (sphere radii)*				Identification	Predicted Position
$a/\lambda_c = 1$	$a/\lambda_c = 2$	$a/\lambda_c = 3$	$a/\lambda_c = 4$		
0.0	0.0	0.0	0.0	front axial	0.0
5.5	5.35			surface wave $N = 1$, $M = 0$ (?)	5.14
7.5	7.45	7.45	7.45	surface wave $N = 1$, $M = 1$	7.41
9.95	9.975	10.00	10.00	rear axial	10.00
18.5	18.45	18.35	18.325	surface wave $N = 2$, $M = 3$	18.22
not resolvable	19.925			axial ray (3 internal reflections)	20.00
20.45	20.525	20.525	20.50	surface wave $N = 2$, $M = 4$	20.48
22.475	22.55				
	29.40			surface wave $N = 3$, $M = 5$	29.03
29.775	29.775				
31.775	31.60	31.475	31.425	surface wave $N = 3$, $M = 6$	31.29
33.65	33.625	33.60	33.575	stationary ray $p = 7$ (?)	33.9
39.125	39.25				
42.575	42.625				
43.10	43.125			bounce ray	
45.10	44.775			surface ray $N = 4$, $M = 9$	44.37
46.725	46.70				

*Due to the calculational increment, the resolution here is 0.025.

Similar results of short pulse calculations for $n = 1.6 + i\,0.01$ are presented in Figs. 24 through 28, and a comparison between the position of the observed and predicted returns is given in Table IX. Again it appears that the predictions agree fairly well with the calculated results; however the lack of better resolution makes it impossible to see all the predicted returns clearly, and may also, due to interferences between returns occurring close together, shift the apparent positions of the maxima.[*] In particular, the rear axial ray and glory ray returns cannot be resolved. The parameters for the calculations presented in Figs. 27 and 28 were the same except for the pulse width. With the slightly increased resolution of Fig. 28 the presence of a second return, believed to be the rear axial return, may be inferred on the leading edge of the largest response, which is probably the glory ray return.

Figure 29 shows the results of some attempts to increase the resolution by decreasing the pulse width, and in Fig. 29(c) the glory ray and the rear axial return can be resolved. These two returns occur at the predicted positions, viz., 6.40a for the rear axial ray and 6.56a for the glory ray.[†] Figure 29 also illustrates some of the drawbacks of the present short pulse synthesis. For the present analysis computed CW scattered amplitudes and phases were available for a/λ ranging from 0.01 to 8.00, in increments of 0.01. As the pulse length is shortened the bandwidth is increased and data for larger values of a/λ are necessary in order to faithfully present the response. In addition, increasing the bandwidth gives more weight to contributions from relatively long wavelengths. These contributions for small values of a/λ are, however, less attenuated for longer optical paths and may appear folded-over on these plots.[‡]

D. Comparison of Predicted and Observed Amplitudes

The amplitude of those ray bundles predicted by geometrical optics, i.e., the returns considered earlier with the exception of the surface waves, is generally of the form[4]

$$A = \frac{1}{2}(\epsilon_1 + \epsilon_2)\sqrt{D} \quad [\S]$$

$$\epsilon_{1,2} = \begin{cases} |r_{1,2}| & p = 0 \\ |(1 - r_{1,2}^2)(-r_{1,2})^{p-1}| & p = 1, 2, 3, \ldots \end{cases}$$

where r_1 and r_2 are the Fresnel reflection coefficients, and D is the divergence.[¶] The quantities ϵ_1^2 and ϵ_2^2 are presented in Tables II and III. The divergence D takes into account various focusing and defocusing effects.

The problem of predicting the amplitudes of the returns is thus primarily that of predicting the divergence or spatial attenuation factor. In the literature this has generally been carried out for only a few of the returns by means of geometrical or physical optics.[37-43] Sometimes corrections, based on various other considerations, are also included. Occasionally one obtains the impression that these methods do not lead to a straightforward method for obtaining this factor,

---

* This is evident, for example, in the results of the measurements presented in Fig. 8.

† For these figures the resolution due to the calculational increments is 0.01a.

‡ See footnote for Eq. (17) on p. 23.

§ The subscript 1 refers to parallel or E-plane polarization and the subscript 2 refers to perpendicular or H-plane polarization.

¶ A quantity related to $\sqrt{D}$ is sometimes called the spatial attenuation factor.[37,52]

Fig. 24. Envelope of short pulse response of dielectric sphere, $n = 1.6 + i0.01$ ($\tau = 0.5a$, $T = 50a$, $a/\lambda_c = 1.0$).

Fig. 25. Envelope of short pulse response of dielectric sphere, $n = 1.6 + i0.01$ ($\tau = 0.5a$, $T = 50a$, $a/\lambda_c = 2.0$).

Fig. 26. Envelope of short pulse response of dielectric sphere, $n = 1.6 + i0.01$ ($\tau = 0.5o$, $T = 50o$, $o/\lambda_c = 3.0$).
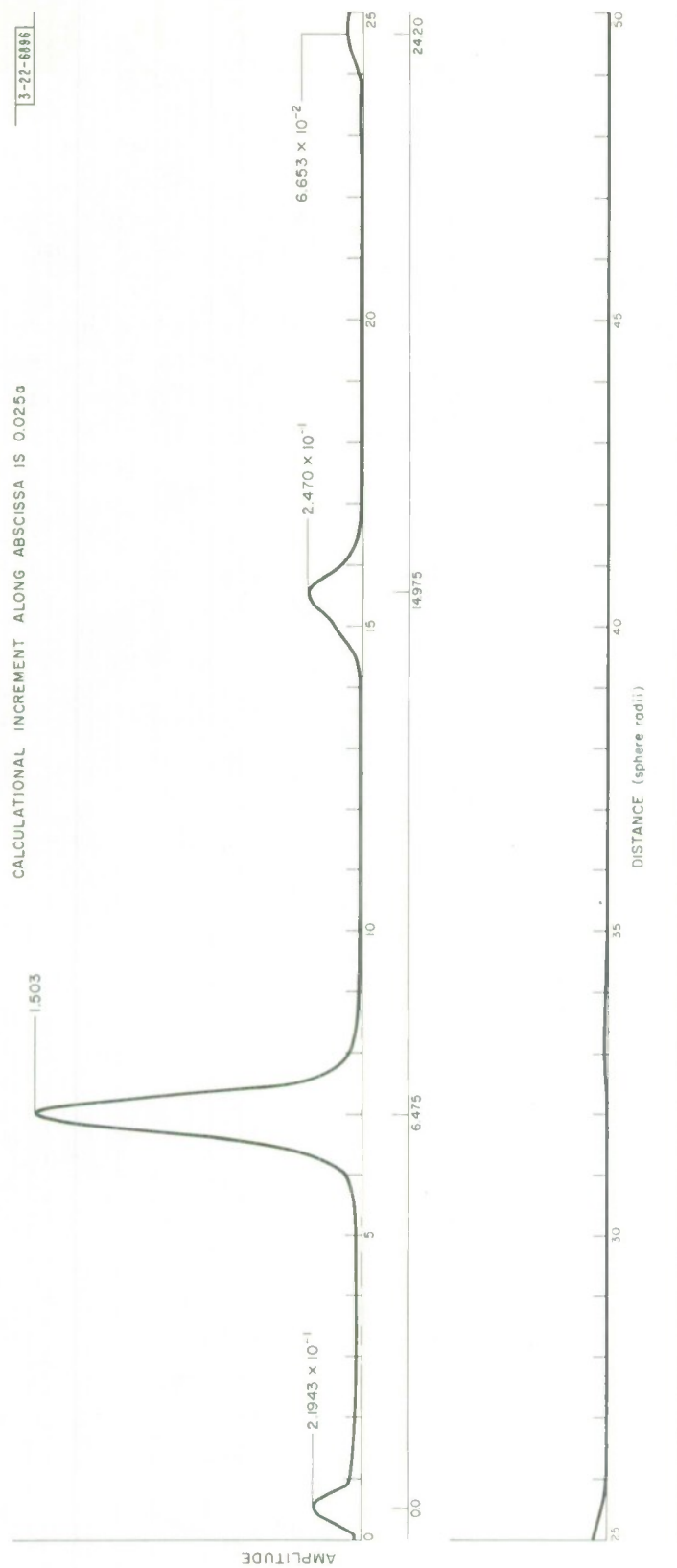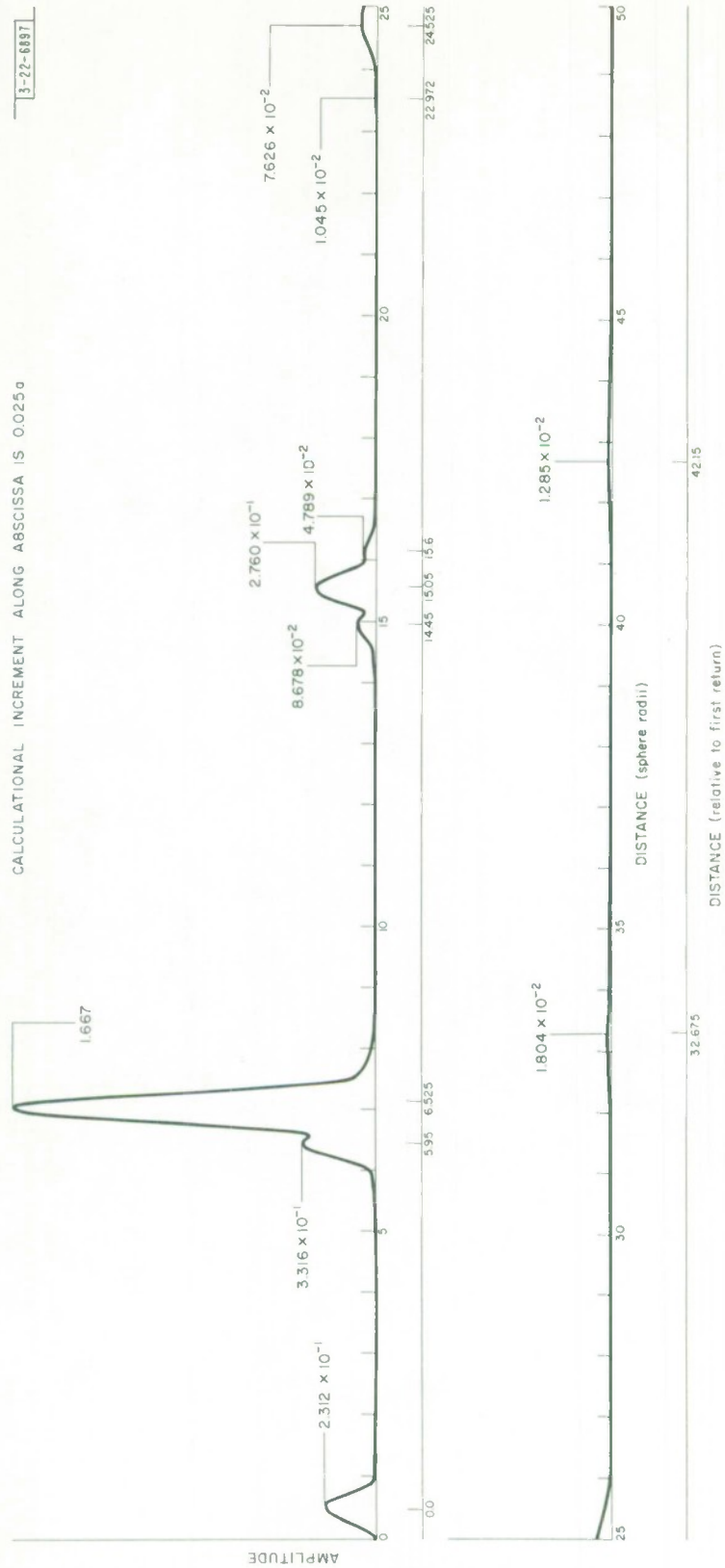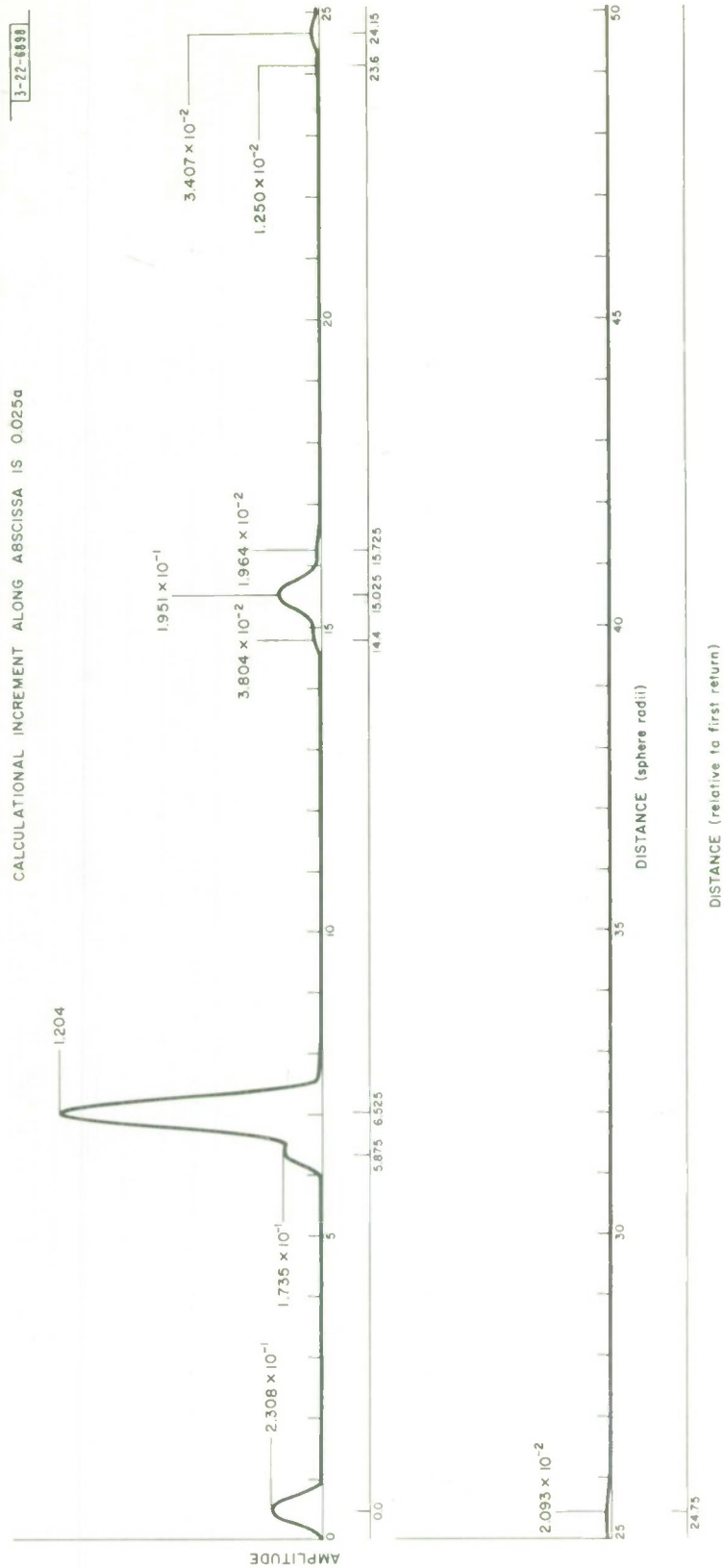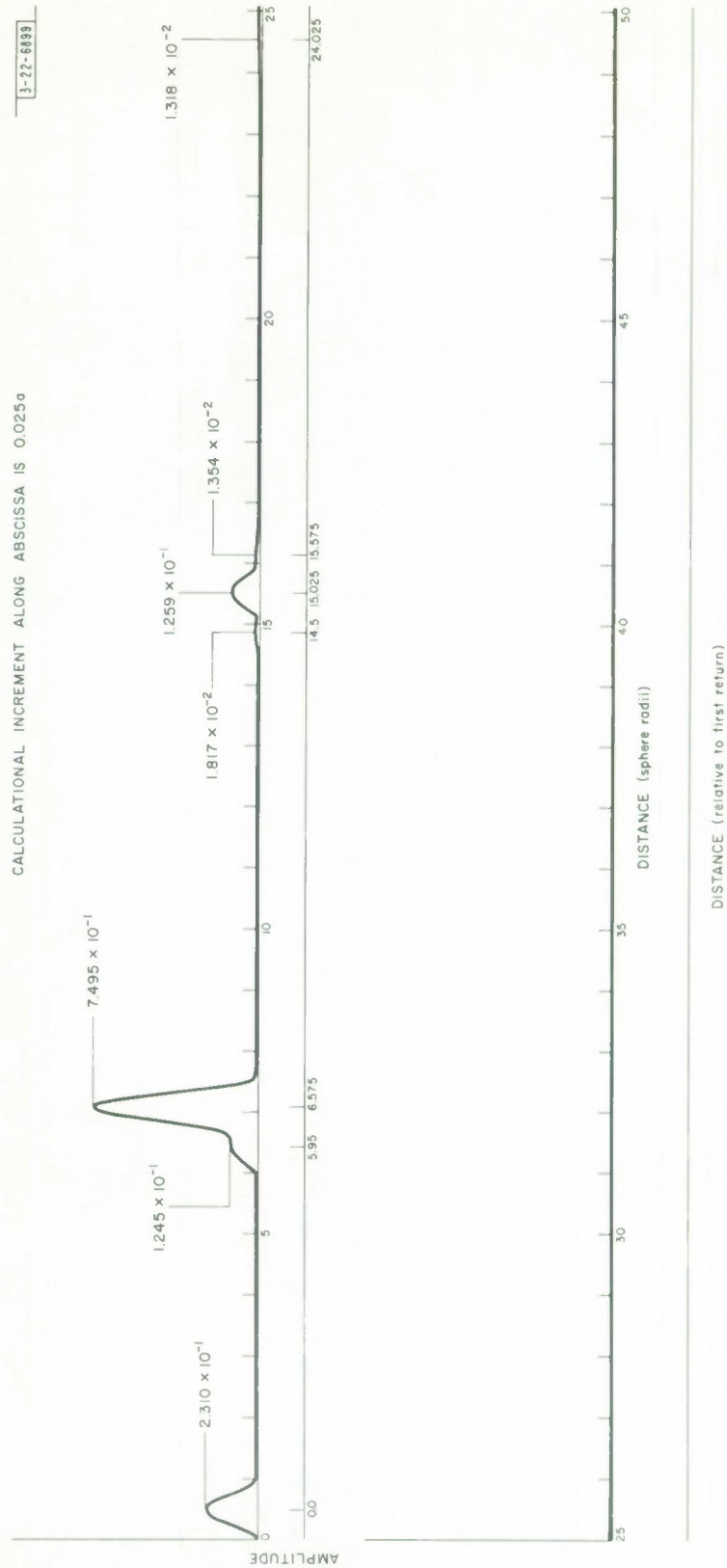
34

Fig. 27. Envelope of short pulse response of dielectric sphere, $n = 1.6 + i0.01$ ($\tau = 0.5a$, $T = 50a$, $a/\lambda_c = 4.0$).
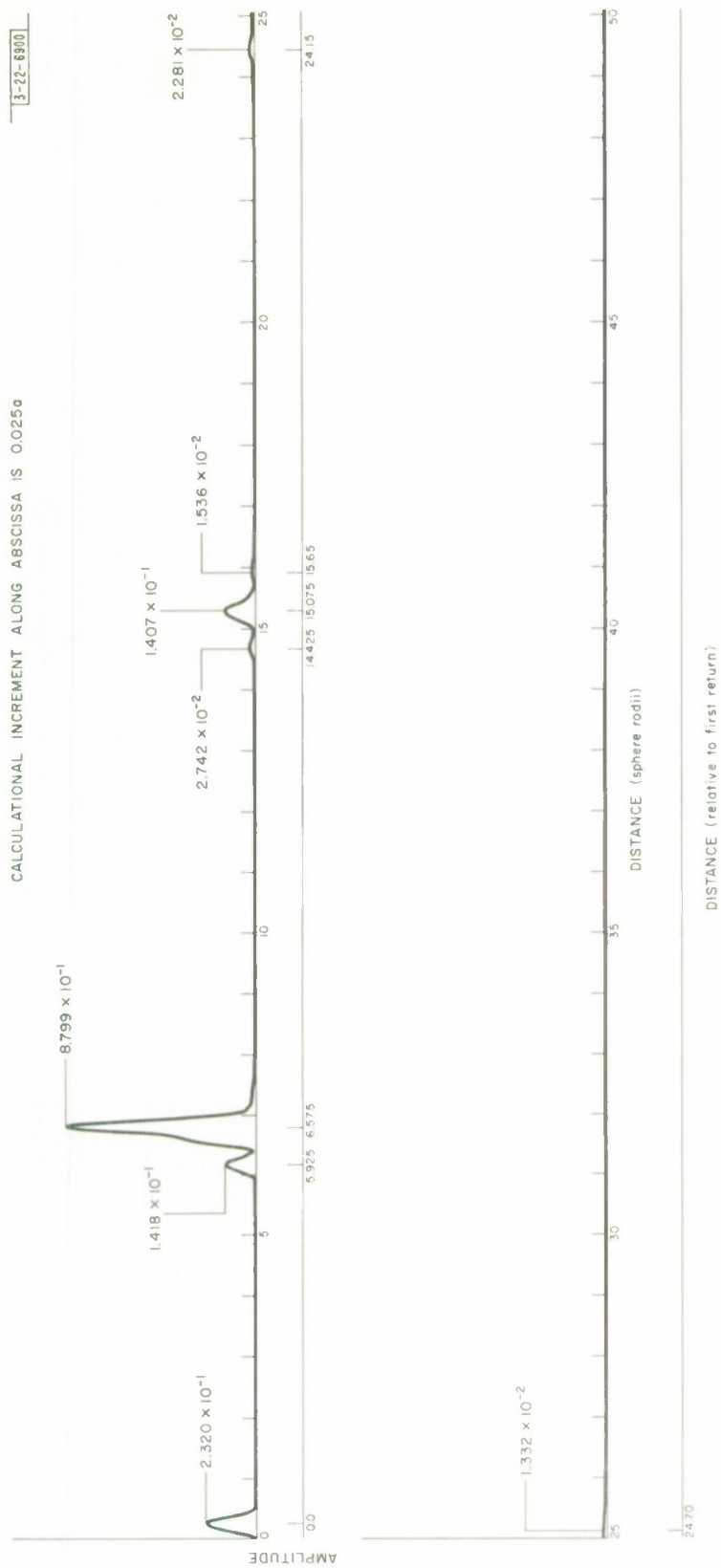
Fig. 28. Envelope of short pulse response of dielectric sphere, $n = 1.6 + i0.01$ ($\tau = 0.25a$, $T = 50a$, $a/\lambda_c = 4.0$).

36

TABLE IX

COMPARISON OF THE POSITION OF THE PREDICTED AND OBSERVED RETURNS, m = 1.6

Position of Observed Return (relative to peak of front axial return) (sphere radii)*					Identification	Predicted Position
$a/\lambda_c = 1$ $\tau = 0.5$	$a/\lambda_c = 2$ $\tau = 0.5$	$a/\lambda_c = 3$ $\tau = 0.5$	$a/\lambda_c = 4$ $\tau = 0.5$	$a/\lambda_c = 4$ $\tau = 0.25$		
0.0	0.0	0.0	0.0	0.0	front axial	0.0
	5.95	5.875	5.95	5.95	surface wave N = 1, M = 1	5.85
					{ stationary ray p = 2 (?)	6.17
6.475	6.525	6.525	6.575	6.575	rear axial	6.40
					bounce ray (glary) N = 1, p = 2	6.56
	14.45	14.40	14.50	14.425	surface wave N = 2, M = 3	13.54
14.975	15.05	15.025	15.025	15.075	{ surface wave N = 2, M = 4	14.25
					bounce ray N = 2, p = 5	14.8
	15.6	15.725	15.757	15.65	surface wave N = 2, M = 5	14.96
	22.975	23.6			surface wave N = 3, M = 6 (?)	21.95
24.20	24.525	24.15	24.025	24.15	surface wave N = 3, M = 7 (?)	22.65
		24.75		24.70	surface wave N = 3, M = 8 (?)	23.36
32.50	32.675				surface wave N = 4, M = 11 or 12 (?)	30 – 32

* Due to the calculational increment the resolution here is 0.025.

CALCULATIONAL INCREMENT ALONG ABSCISSA IS 0.01a

$\tau = 0.25a$

8.822 × 10⁻¹

(a)

2.319 × 10⁻¹

1.424 × 10⁻¹

0   1   2   3   4   5   6   7   8   9   10

0.0   5.91 6.57

AMPLITUDE

$\tau = 0.20a$

8.880 × 10⁻¹

(b)

2.303 × 10⁻¹

1.478 × 10⁻¹

0   1   2   3   4   5   6   7   8   9   10

0.0   5.93 6.56

$\tau = 0.15a$

8.860 × 10⁻¹

REAR AXIAL RAY   GLORY RAY

4.610 × 10⁻¹

(c)

2.220 × 10⁻¹

1.595 × 10⁻¹

0   1   2   3   4   5   6   7   8   9   10

DISTANCE (sphere radii)

0.0   5.94 6.56
                                  6.40
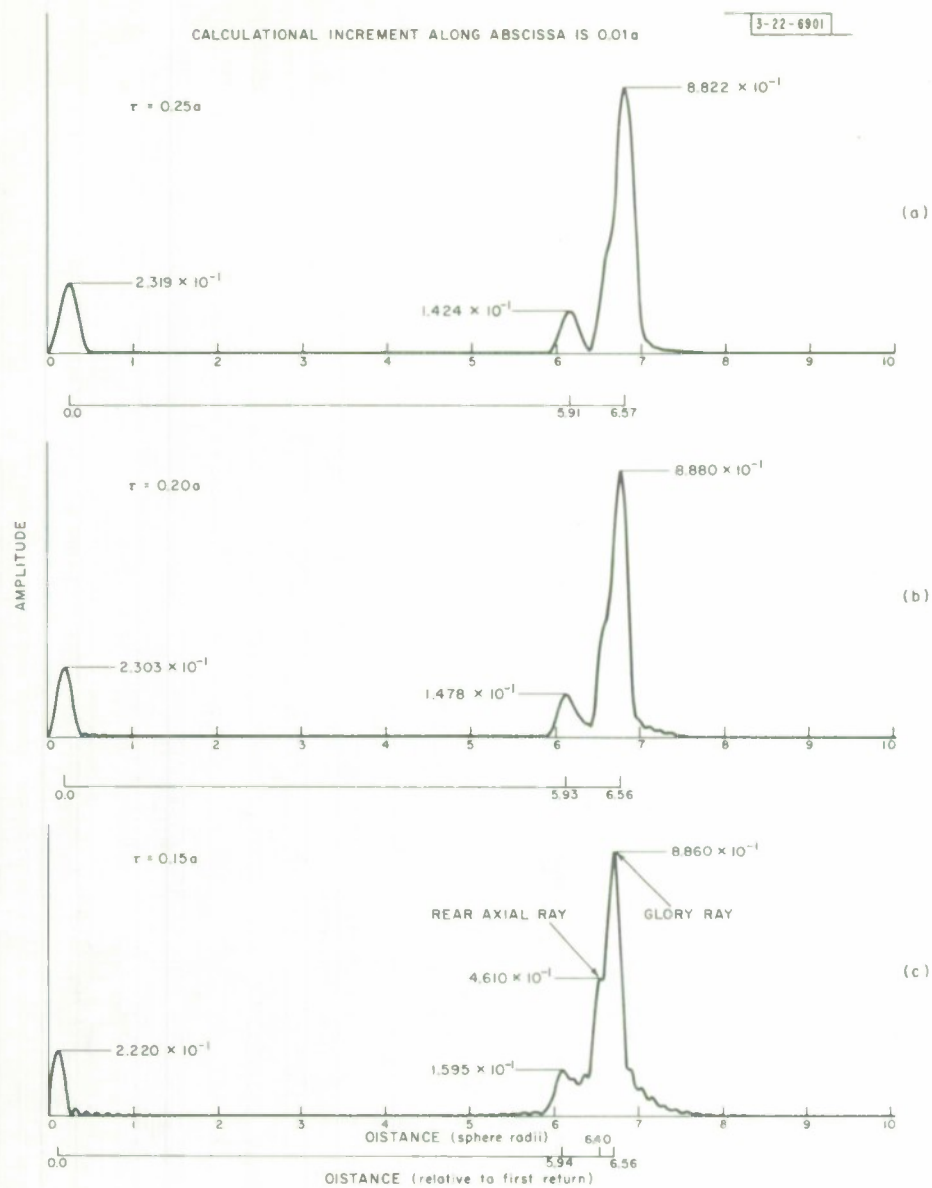
DISTANCE (relative to first return)

Fig. 29(a–c).   Envelope of first part of short pulse response of dielectric sphere, $n = 1.6 + i0.01$, with increasing resolution ($T = 50a$, $a/\lambda_c = 4.0$).

and thus a feeling that the techniques are not as satisfactory as would be desired is obtained. The situation does not appear to be clear, and requires further work.

Utilizing the same general techniques as in his work on the cylinder,[53,54] Kodis,* in some as yet unpublished work, has obtained formulae for the amplitudes of all of the axial and bounce optics rays scattered by a dielectric sphere. This work employs asymptotic, stationary phase, evaluations of the Mie series. The amplitudes obtained by Kodis for the front axial, rear axial and glory rays agree with the formulae presented by Atlas and Glover,[43] which are based in part on the work of Thomas[38,39] and others. In the case of the glory ray there is, however, some difference in the phase of the return. Figure 30 presents the amplitude of the rear axial and glory ray returns as predicted by Atlas and Glover.†
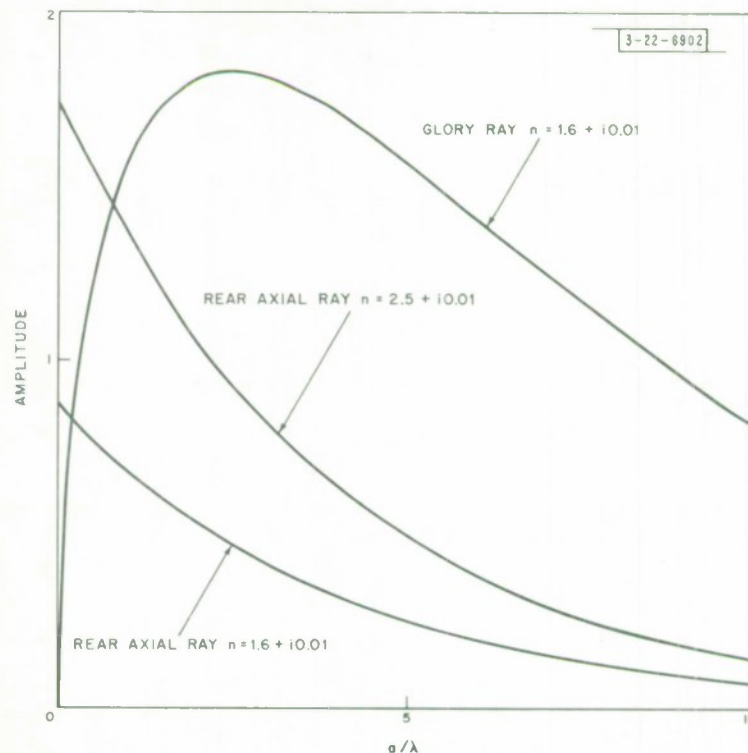

Fig. 30. Amplitude of rear axial and glory ray returns as predicted by Atlas and Glover.[43]

In order to obtain some indication of the agreement between the predicted amplitudes and those observed from the short pulse response, some calculations were carried out in which a short pulse was synthesized using the predicted amplitudes and phases presented by Atlas and Glover, rather than those obtained from the Mie series. Only the front axial, rear axial and glory ray returns were considered. A typical result for $n = 2.5 + i0.01$ is presented in Fig. 31,

---

* Personal communication.

† The amplitudes, taken from Table I of Ref. 43, are:

Front axial $A = (m - 1)/(m + 1)$

Rear axial $A = |\,[4m(m - 1)/(m + 1)^3]\,[m/(2 - m)]\,|\,e^{-4a\kappa}$

Glory $A = 1.5\sqrt{\pi/2}\,|\,m^2(m^2 - 4)(m^2 - 2)^{3/2}/(m^2 - 1)^3\,|\,\sqrt{a}\,e^{-2m\kappa a}$
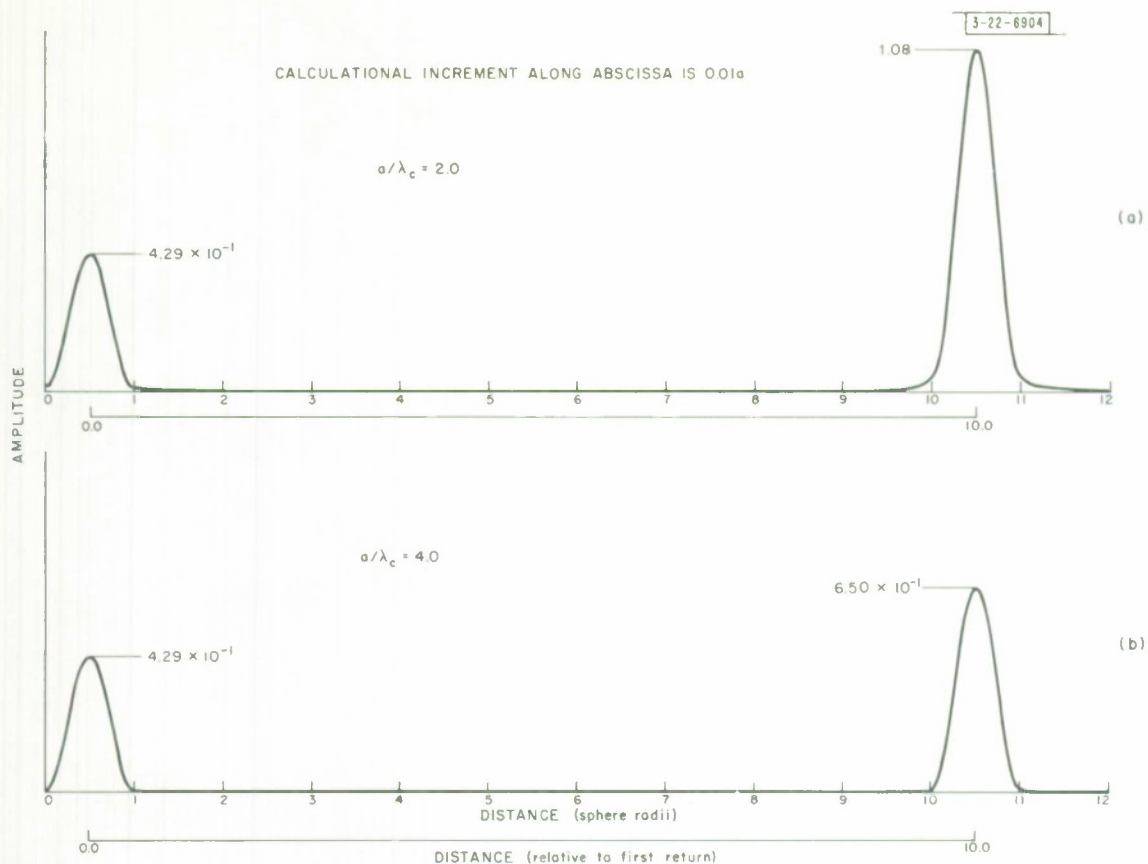
where $a = 2\pi a/\lambda$.

Fig. 31(a,b). Envelope of short pulse response, $n = 2.5 + i0.01$, using amplitudes and phases predicted by Atlas and Glover ($\tau = 0.5a$, $T = 50a$).

and for $n = 1.6 + i0.01$ in Fig. 32. As before, the rear axial ray and the glory ray are not resolvable for $m = 1.6$, however the return due to the rear axial ray is also indicated. These figures may be compared with Figs. 20 through 28. A comparison of the peaks of the returns observed using the optics predictions and the Mie series calculations is given in Table X. The parameters τ, T, and the truncation point of the series are the same for both cases. In order to obtain the amplitude of the rear axial ray for $n = 1.6 + i0.01$, a series of calculations using the optics predictions was carried out in which the glory ray return was not included.

Except for the glory ray return, the agreement does not appear to be bad, particularly when it is remembered that the optics amplitudes were employed even for small values of a/λ. At present the cause for the discrepancy in the case of the glory ray is not apparent. It appears that further work is required in this area.

V. DIELECTRIC COATED CONDUCTING SPHERES

Figures 33 and 34 present the CW backscatter cross section vs a/λ for conducting spheres with relatively thin dielectric coatings. In these figures δ is the fractional thickness of the coating, i.e., $a\delta$ is the thickness of the coating and $a(1 - \delta)$ is the radius of the conducting core, where a is the outer radius of the composite sphere. A comparison with Fig. 1[*] indicates that the presence of such a thin coating changes the character of the curve considerably. Figures 33

---

[*] Note that the ordinate scale of Fig. 1 is linear, while that of Figs. 33 and 34 is logarithmic.

40

$a/\lambda_c = 2.0$

CALCULATIONAL INCREMENT ALONG ABSCISSA IS 0.01a

— — — REAR AXIAL RETURN
(not resolvable from
glory ray)

(a)

1.82×10^0

5.37×10^{-1}

2.31×10^{-1}

AMPLITUDE

0   1   2   3   4   5   6   7   8

0.0   6.40 6.53

$a/\lambda_c = 4.0$

CALCULATIONAL INCREMENT ALONG ABSCISSA
IS 0.01a

— — — REAR AXIAL RETURN
(not resolvable from
glory ray)

(b)

1.78×10^0

3.25×10^{-1}

2.31×10^{-1}

0   1   2   3   4   5   6   7   8
DISTANCE (sphere radii)

0.0   6.40 6.54
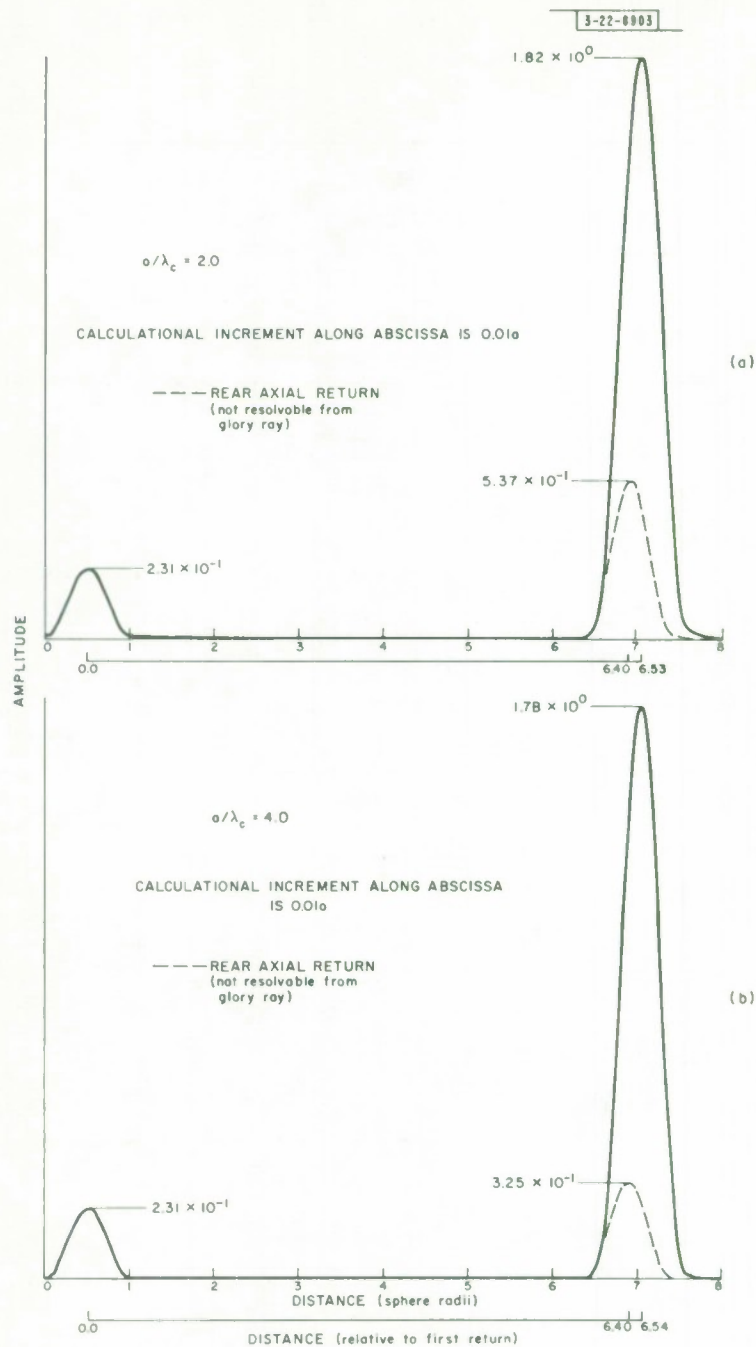DISTANCE (relative to first return)

Fig. 32(a,b). Envelope of short pulse response, $n = 1.6 + i0.01$, using amplitudes and phases predicted by Atlas and Glover ($\tau = 0.5a$, $T = 50a$).

41

TABLE X

COMPARISON BETWEEN THE PEAK AMPLITUDES A* OBTAINED USING EITHER OPTICS
PREDICTIONS OR MIE SERIES CALCULATIONS AS THE INPUT FOR THE
SHORT PULSE CALCULATIONS

a/λ_c †	Front Axial Ray		Rear Axial Ray		Glary Ray	
	Optics	Mie Series	Optics	Mie Series	Optics	Mie Series
n = 1.6 + i0.01						
1.0	0.231	0.219	0.678		1.20	1.50
2.0	0.231	0.231	0.537		1.82	1.67
3.0	0.231	0.231	0.417	nat resalvable	1.95	1.20
4.0 τ = 0.5a	0.231	0.319	0.325		1.78	0.749
τ = 0.25a	0.232	0.232	0.342			0.882
τ = 0.20a	0.231	0.230	0.354			0.888
τ = 0.15a	0.226	0.222	0.364	~ 0.461	1.47	0.886
n = 2.5 + i0.01						
1.0	0.429	0.409	1.36	1.12	The glary ray does nat exist far m = 2.5	
2.0	0.429	0.430	1.08	1.30		
3.0	0.429	0.429	0.835	0.821		
4.0	0.429	0.428	0.650	0.644		

* The units are such that $\sigma/\pi a^2 = A^2$.

† Unless atherwise nated, $\tau = 0.5a$.
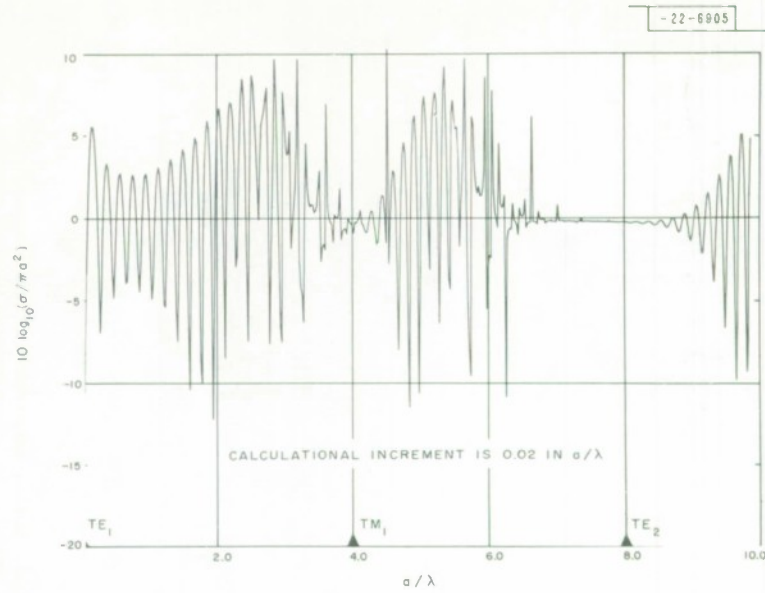
Fig. 33. Backscatter cross section of dielectric coated conducting sphere, m = 1.6, δ = 0.05.
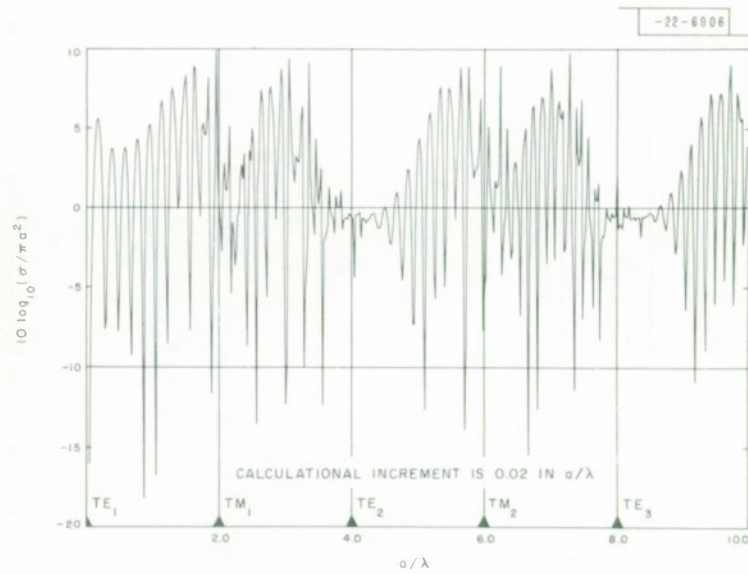

Fig. 34. Backscatter cross section of dielectric coated conducting sphere, m = 1.6, δ = 0.10.

and 34, together with other similar data, have been published previously.[55][*] At that time a comparison was made with a creeping wave analysis by Helstrom,[57-59] and an attempt was made to explain the basic features of these figures in terms of creeping waves.

Heuristically, the model for scattering from a conducting sphere with a thin dielectric coating is that, as in the case of the conducting sphere, there exists a specular return and a creeping wave return. The specular return is effectively the same in each case except that for the coated sphere interference effects may arise due to rays reflected at the free-space dielectric interface and the dielectric conductor interface. Creeping waves are also launched which circumnavigate the sphere one or more times. On conducting spheres, because of the attenuation due to radiation, generally only the first creeping wave, that which has completed a half revolution around the sphere, has an appreciable magnitude and even this becomes negligible for $a/\lambda > 1$. Under some conditions for coated spheres the situation is similar; it is different, however, when the condition

$$2\delta(a/\lambda)(m-1)^{1/2} \geqslant \begin{cases} \ell - 1 & \text{TE}_\ell \text{ mode} \\ \ell - 1/2 & \text{TM}_\ell \text{ mode} \end{cases} \qquad \ell = 1, 2, 3, \ldots \qquad (18)$$

obtains. The creeping waves of the given mode are then propagated with decreasing attenuation. The triangles along the axis of abscissas of Figs. 33 and 34 indicate when the equality of Eq. (18) is satisfied, and at these points the "bursts" of oscillations begin to become apparent. The apparent end of each "burst" as seen in the figures is, however, misleading since it is due to the size of the increment in a/λ (0.02) with which these curves were computed. It is believed that the resonances continue with increasing a/λ, but that they are not apparent because of the monotonically increasing Q (i.e., decreasing width) of the resonances. Even carrying out calculations with much smaller increments in a/λ may not be sufficient to obtain a smooth curve which shows all of the fine structure.[†]

When the conditions of Eq. (18) are satisfied, the form of the equation for the backscattered amplitude of the creeping wave contribution, as derived by Helstrom, is quite similar to the form which obtains when waves are trapped in a dielectric coating on a plane perfectly conducting surface. Rays may be considered as propagating by repeated reflections at the dielectric-free space and dielectric-conductor interfaces. The reflection coefficient at the latter interface is unity and when the equality in Eq. (18) is satisfied the reflection coefficient at the dielectric-free space interface is also unity, i.e., the angle of incidence is the critical angle for total internal reflection α_c. These waves do not appear, however, to have the same character as the surface waves observed on dielectric spheres. When Eq. (18) is satisfied but moves away from the equality the angle of incidence α becomes larger than α_c, so that surface waves of the character considered earlier do not appear possible, unless the coating is considerably thicker.

Typical examples of the short pulse response of a coated sphere are shown in Figs. 35[‡] through 37. Here the reference is taken to be the front surface of the composite sphere. The specular return has its peak response roughly at the distance $2m\delta a$, corresponding to reflection from the conducting core. In addition, the presence of several creeping wave returns, corresponding to pulses which have circumnavigated the sphere one or more times, are indicated.

---

* Reference 56 presents similar data for conducting spheres with a thin lossy dielectric coating.

† This is demonstrated in Figs. 8 through 10 of Ref. 55.

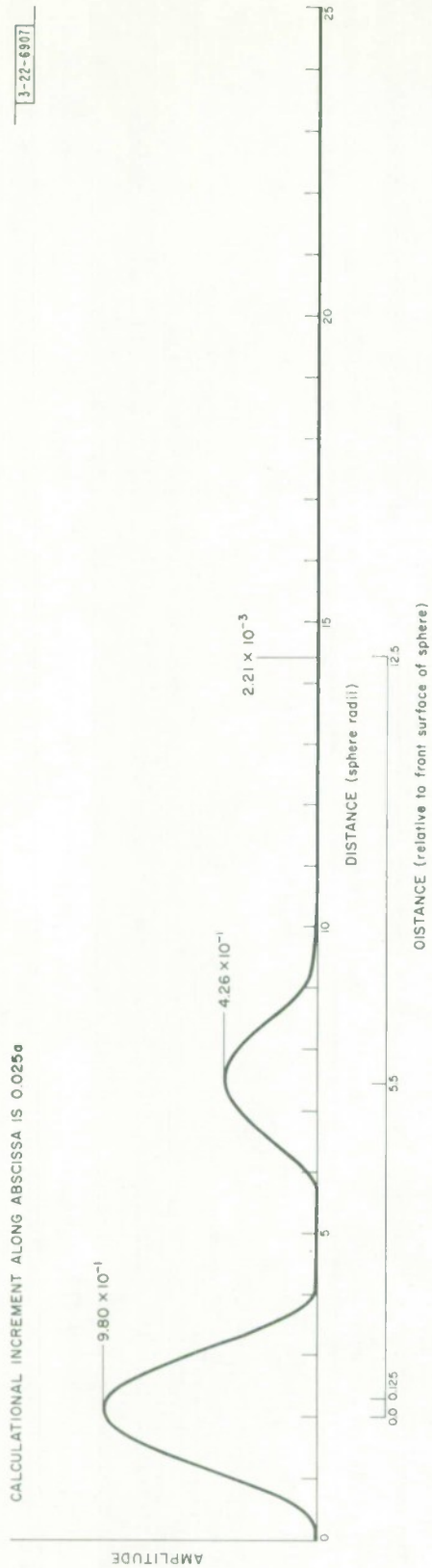‡ Other examples are shown in Ref. 60.

CALCULATIONAL INCREMENT ALONG ABSCISSA IS 0.025a

9.80×10^{-1}

4.26×10^{-1}

2.21×10^{-3}

AMPLITUDE

DISTANCE (sphere radii)

OISTANCE (relative to front surface of sphere)

0.0 0.125

Fig. 35. Envelope of short pulse response from coated sphere, $m = 1.6$, $\delta = 0.5$ ($\tau = 2.0a$, $T = 50a$, $a/\lambda_c = 1.0$).

CALCULATIONAL INCREMENT ALONG ABSCISSA IS 0.025a

9.65×10^{-1}

1.62×10^{0}

5.70×10^{-2}

4.66×10^{-3}

AMPLITUDE

DISTANCE (sphere radii)

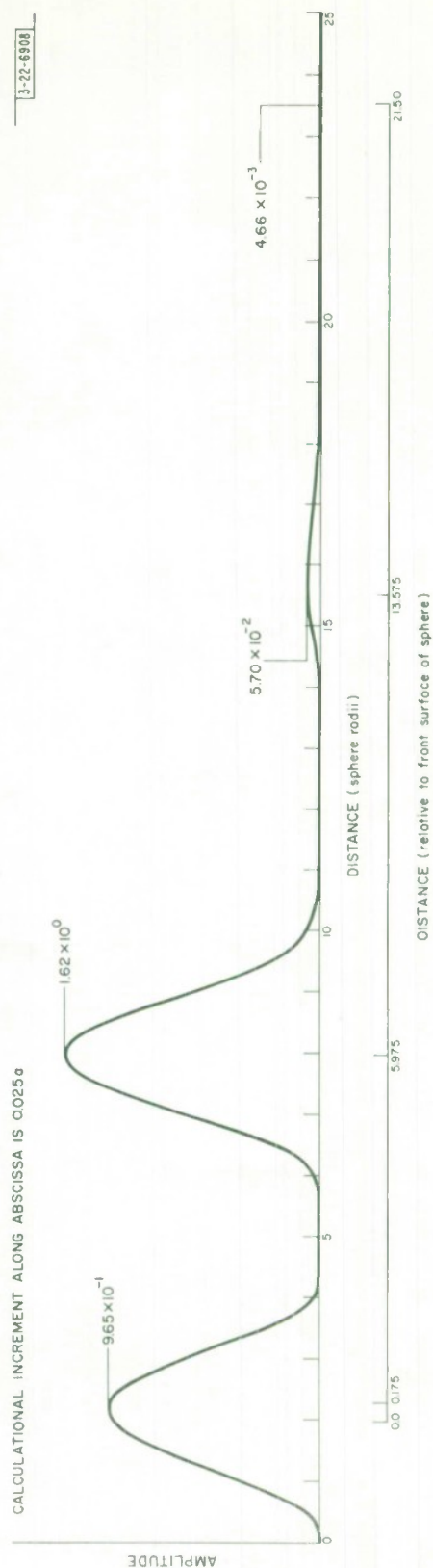OISTANCE (relative to front surface of sphere)

0.0 0.175

5.975

13.575

21.50

Fig. 36. Envelope of short pulse response fram coated sphere, $m = 1.6$, $\delta = 0.5$ ($\tau = 2.0a$, $T = 50a$, $a/\lambda_c = 2.0$).
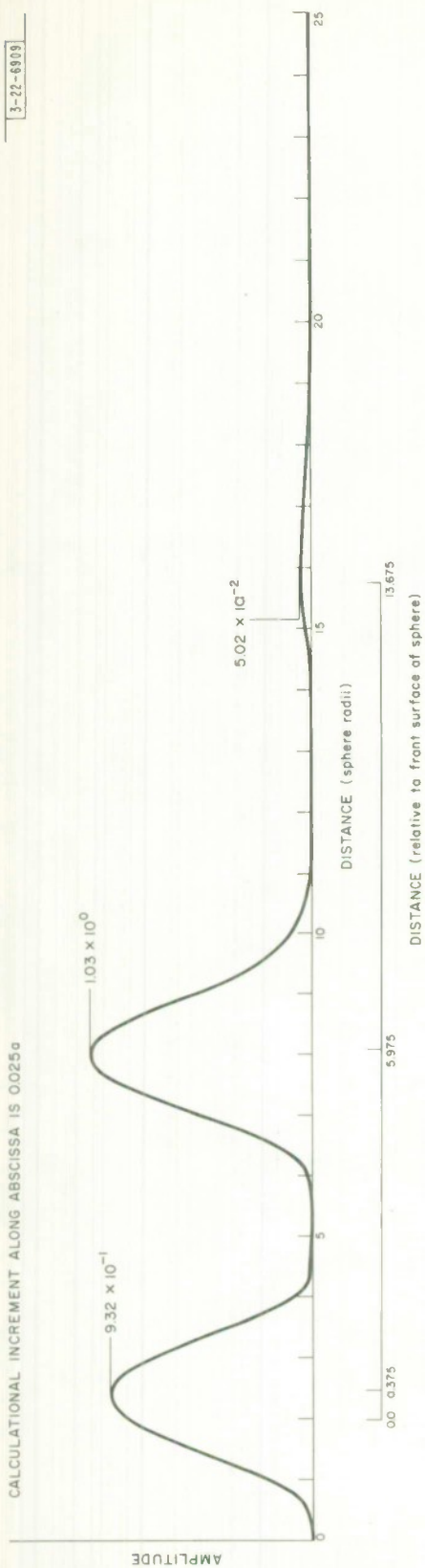
45

CALCULATIONAL INCREMENT ALONG ABSCISSA IS 0.025a

Fig. 37. Envelope of short pulse response from coated sphere, m = 1.6, δ = 0.1 (τ = 2.0a, T = 50a, a/λ$_c$ = 1.0).

CALCULATIONAL INCREMENT ALONG ABSCISSA IS 0.025a
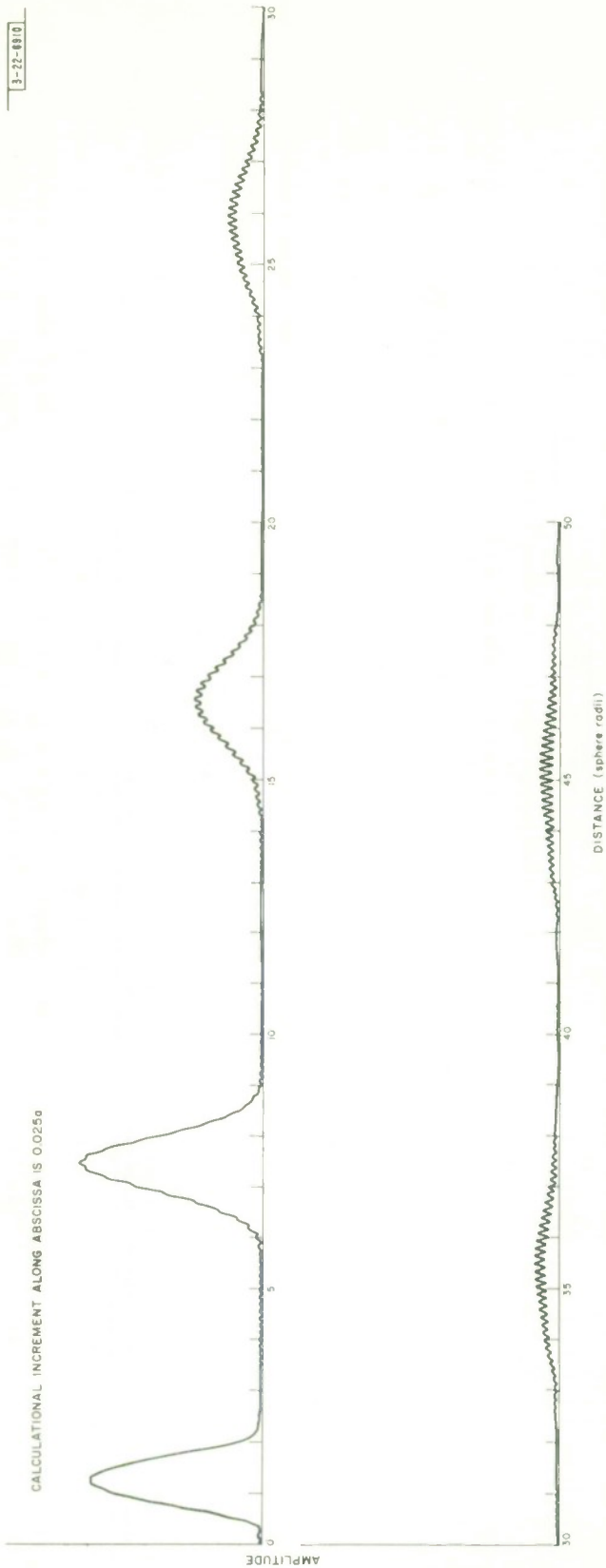

Fig. 38. Envelope of short pulse response from coated sphere m = 1.6, δ = 0.05, illustrating effects due to insufficiently fine sampling of amplitudes and phases of CW return (τ = 2.0a, T = 50a, a/λ$_c$ = 3.0).

46

Because the increment in a/λ (0.01) at which the Mie series calculations were carried out for these figures is not sufficiently small to sample all the fine structure of the return, the results obtained by increasing the resolution, i.e., the bandwidth, or decreasing the carrier wavelength, become less meaningful, as shown in Fig. 38. However, the presence of a series of creeping waves is still apparent.

While no quantitative comparison has been carried out here, these examples of the short pulse response of a coated sphere are consistent with the creeping wave model briefly described above. As the thickness of the coating is increased, the number of expected returns increases very quickly. Not only are returns of the type seen in Figs. 34 and 35 expected, but also various optics returns,[37,40,53] and surface wave returns of the type described in Sec. IV on dielectric spheres.

VI. CONCLUSION

In this report the backscatter from spheres in the time domain has been considered. It is hoped that this survey of an old problem from a viewpoint different from previous approaches will be of value in improving our knowledge of the phenomena involved. Although the sphere itself is only of limited interest it is believed that an examination of the short pulse response may aid in the development and application of various approximate models to scatterers of interest for which rigorous solutions are not available.

The results presented indicate the backscatter from conducting spheres is well understood, and that our knowledge of the phenomena involved is good. The model in which the backscatter consists primarily of two returns, viz., the specular and the creeping wave returns, appears to be well substantiated both qualitatively and quantitatively. The short pulse results also show that the model is valid for smaller values of a/λ than was previously supposed.

The backscatter from dielectric spheres does not appear to be as well understood. The results of the short pulse study indicate the presence of the optics returns predicted by simple ray tracing arguments; however there appears to be a discrepancy between the predicted amplitude and that observed in the short pulse response for one of the returns, viz., the glory ray. The short pulse response also indicated the presence of a series of returns not predicted by geometrical optics. It is believed that these returns are due to surface waves which may take short cuts through the sphere, entering and leaving the sphere at the critical angle of internal reflection. It appears that further study is necessary to improve our understanding not only of these surface waves, but of the optics rays as well.

The scattering from conducting spheres with a relatively thin dielectric coating appears to be only qualitatively understood. The presence of a specular return and a series of creeping wave returns seems to be verified; however, at present few quantitative statements can be made.

ACKNOWLEDGMENTS

REFERENCES

1. N. A. Logan, "Survey of Some Early Studies of the Scattering of Plane Waves by a Sphere," Proceedings of the IEEE 53, 773-785 (1965).

2. H. A. Corriher, Jr., and B. O. Pyron, "A Bibliography of Articles on Radar Reflectivity and Related Subjects: 1957-1964," Proceedings of the IEEE 53, 1025-1064 (1965).

3. J. Rheinstein, "Scattering of Electromagnetic Waves by an Eaton Lens," Technical Report 273, Lincoln Laboratory, M. I. T. (June 1962), DDC 289380.

4. H. C. Van de Hulst, Light Scattering by Small Particles (John Wiley and Sons, Inc. New York, 1957).

5. J. B. Keller, "A Geometrical Theory of Diffraction," New York University, Institute of Mathematical Sciences, Division of Electromagnetic Research Report EM-115 (July 1958), AD 152454.

6. _____, "Geometrical Theory of Diffraction," Journal of the Optical Society of America 52, 116-130 (1962).

7. W. Franz, Theorie der Beugung Elektromagnetischer Wellen (Springer Verlag, Berlin, 1957).

8. W. Franz and K. Klante, "Diffraction by a Surface of Variable Curvature," IRE Transactions on Antennas and Propagation AP-7, S68-S70 (1959).

9. R. F. Goodrich, "Fock Theory, an Appraisal and Exposition," IRE Transactions on Antennas and Propagation AP-7, S28-S36 (1959).

10. V. A. Fock, Electromagnetic Diffraction and Propagation Problems (Pergamon Press, New York, 1965).

11. J. W. Crispin and A. L. Maffett, "Radar Cross-Section Estimation for Simple Shapes," Proceedings of the IEEE 53, 833-848 (1965).

12. T. B. A. Senior, "A Survey of Analytical Techniques for Cross-Section Estimation," Proceedings of the IEEE 53, 822-833 (1965).

13. T. B. A. Senior and R. F. Goodrich, "Scattering by a Sphere," Proceedings of the IEEE (British) 111, 907-916 (1964).

14. E. M. Kennaugh and R. L. Cosgriff, "The Use of the Impulse Response in Electromagnetic Scattering Problems," 1958 IRE National Convention Record, Part 1, p. 72-77.

15. E. M. Kennaugh, "The Scattering of Transient Electromagnetic Waves by Finite Bodies," Antenna Laboratory, Ohio State University Research Foundation, Final Engineering Report 1073-4, 20-41 (January 1961), AD 255839.

16. _____, "The Scattering of Electromagnetic Pulses by a Conducting Sphere," Proceedings of the IRE 49, 380 (1961).

17. E. M. Kennaugh and D. L. Moffatt, "On the Axial Echo Area of the Cone-Sphere Shape," Proceedings of the IRE 50, 199 (1962).

18. _____, "The Axial Echo Area of a Perfectly Conducting Prolate Spheroid," Antenna Laboratory, The Ohio State University Research Foundation Report 1774-1 (June 1964).

19. _____, "Transient and Impulse Approximations," Proceedings of the IEEE 53, 893-901 (1965).

20. D. L. Moffatt and E. M. Kennaugh," The Axial Echo Area of a Perfectly Conducting Prolate Spheroid," IEEE Transactions on Antennas and Propagation AP-13, 401-409 (1965).

21. J. R. Wait, "Diffraction of a Spherical Wave Pulse by a Half-Plane Screen," Canadian Journal of Physics 31, 693-696 (1957).

22. F. G. Friedlander, <u>Sound Pulses</u> (Cambridge University Press, 1958).

23. V. H. Weston, "Pulse Return from a Sphere," IRE Transactions on Antennas and Propagation <u>AP-7</u>, 543-551 (1959).

24. W. J. Welch, "A Variational Solution for the Scattering of Electromagnetic Pulses from a Cylinder of Finite Length," Electronics Research Laboratory, University of California, Berkeley, Institute of Engineering Research, Series 60, Issue 392 (August 1961), AD 265-853.

25. W. E. Williams, "Refraction and Diffraction of Pulses," Canadian Journal of Physics <u>39</u>, 272-275 (1961).

26. D. E. Foreman and D. F. Sedivec, "Experimental Observation of the Creeping-Wave Phenomenon in Backscatter Using a Short-Pulse Radar System," Proceedings of the IEEE <u>53</u>, 1102-1104 (1965).

27. A. V. Alongi, R. E. Kell and D. J. Newton, "A High Resolution X-Band FM/CW Radar for RCS Measurements," Proceedings of the IEEE <u>53</u>, 1072-1076 (1965).

28. R. Hickling, "Analysis of Echoes from a Solid Elastic Sphere in Water," Journal of the Acoustical Society of America <u>34</u>, 1582-1592 (1962).

29. _____, "Analysis of Echoes from Hollow Metallic Spheres in Water," Journal of the Acoustical Society of America <u>36</u>, 1124-1137 (1964).

30. H. Überall, R. D. Doolittle and J. V. McNicholas, "Use of Sound Pulses for a Study of Circumferential Waves," Journal of the Acoustical Society of America <u>39</u>, 564-578 (1966).

31. R. D. Stuart, <u>An Introduction to Fourier Analysis</u> (John Wiley and Sons, Inc. New York, 1961).

32. D. Atlas, L. J. Battan, W. G. Harper, B. M. Herman, M. Kerker, and E. Matijevic, "Backscatter by Dielectric Spheres (Refractive Index ~1.6)," IEEE Transactions on Antennas and Propagation <u>AP-11</u>, 68-72 (1963).

33. J. Rheinstein, "Tables of the Amplitude and Phase of the Backscatter from a Conducting Sphere (Radius/Wavelength = 0.01 to 19.00 in Steps of 0.01)," Group Report 22G-16, Lincoln Laboratory, M. I.T. (June 1963), DDC 409820.

34. N. A. Logan, "Scattering Properties of Large Spheres," Proceedings of the IEEE <u>48</u>, 1782 (1960).

35. J. H. Pannell, J. Rheinstein and A. F. Smith, "Radar Scattering from a Conducting Cone-Sphere," Technical Report 349, Lincoln Laboratory, M. I. T. (2 March 1964), DDC 600411.

36. T. B. A. Senior, "The Backscattering Cross Section of a Cone-Sphere," IEEE Transactions on Antennas and Propagation <u>AP-13</u>, 271-277 (1965).

37. L. Peters, Jr., T. Kawana and W. G. Swarner, "Approximations for Dielectric or Plasma Scatterers," Proceedings of the IEEE <u>53</u>, 882-892 (1965).

38. D. T. Thomas, "Approximation for Backscatter from Dielectric Spheres," Antenna Laboratory, Ohio State University Research Foundation Report 1116-14 (October 1961).

39. _____, "Scattering by Plasma and Dielectric Bodies," Antenna Laboratory, Ohio State University Research Foundation Report 1116-2 (August 1962).

40. W. G. Swarner and L. Peters, Jr., "Radar Cross Sections of Dielectric or Plasma Coated Conducting Spheres and Circular Cylinders," IEEE Transactions on Antennas and Propagation <u>AP-11</u>, 558-569 (1963).

41. R. G. Kouyoumjian, L. Peters, Jr., and D. T. Thomas, "A Modified Geometrical Optics Method for Scattering by Dielectric Bodies," IEEE Transactions on Antennas and Propagation <u>AP-11</u>, 690-703 (1963).

42. J. R. Hodkinson and I. Greenleaves, "Computation of Light-Scattering and Extinction According to Diffraction and Geometrical Optics, and Some Comparisons with the Mie Theory," Journal of the Optical Society of America 53, 577-588 (1963).

43. D. Atlas and K. M. Glover, "Backscatter by Dielectric Spheres With and Without Metal Caps," in Proceedings of the Inter-Disciplinary Conference on Electromagnetic Scattering, M. Kerker, editor, Potsdam, N. Y., 13-16 August 1962 (Pergamon Press, New York, 1962), pp. 213-236.

44. F. Goos and H. Hänchen, "Ein neuer und fundamentaler Versuch zur Totalreflexion," Annalen der Physik 6. folge 1, 333-346 (1947).

45. H. Maecker, "Quantitativer Nachweis van Grenzschichtwellen in der Optik," Annalen der Physik 6. folge 4, 409-431 (1949).

46. K. Artman, "Brechungund Reflexion einer seitlich begrenzten (Licht-) Welle an der ebenen Trenn fl ä che zweier Medien in Nähe des Grenzwinkels der Totalreflexion," Annalen der Physik 6. folge 8, 270-284 (1951).

47. H. Maecker, "Die Grenze der Totalreflexion II. Strenge welloptische Berechnung," Annalen der Physik 6. folge 10, 153-160 (1952).

48. G. Lehman und H. Maecker, "Die Grenze der Totalreflexian III. Experimentelle Nachprüfung," Annalen der Physik 6. folge 10, 161-166 (1952).

49. K. Artman, "Unter welchen Bedingungen ist der Amplitudenverlauf einer seitlich begrenzten Welle komplex," Annalen der Physik 6. folge 15, 1-5 (1955).

50. P. Beckmann and W. Franz, "Über die Greensche Funktion transparenter Zylinder," Zeitschrift für Naturfarschung 12a, 257-267 (1957).

51. E. G. Reick, "Intensity Distribution af Light Leaving a Hemicylinder," in Proceedings of the Symposium on Quasi-Optics, J. Fax, editar, New Yark, 8-10 June 1964 (Palytechnic Press, Polytechnic Institute of Brooklyn, N. Y., 1964), pp. 545-562.

52. R. G. Kouyoumjian, "Asymptotic High-Frequency Methods," Proceedings of the IEEE 53, 864-876 (1965).

53. R. D. Kodis, "The Scattering Cross Section af a Camposite Cylinder, Geometric Optics," IEEE Transactions an Antennas and Propagation AP-11, 86-93 (1963).

54. W. Streifer and R. D. Kodis, "On Scattering of Electromagnetic Waves by a Dielectric Cylinder," Quarterly af Applied Mathematics 22, 193-206 (1964).

55. J. Rheinstein, "Scattering af Electromagnetic Waves from Dielectric Coated Conducting Spheres," IEEE Transactions on Antenna and Propagation AP-12, 334-340 (1964).

56. _____, "Scattering af Electromagnetic Waves from Conducting Spheres With Thin Lossy Coatings," IEEE Transactions on Antennas and Propagatian AP-13, 983 (1965).

57. C. W. Helstrom, "Scattering from a Cylinder with a Dielectric Coating," Westinghouse Research Laboratories, Scientific Paper, 806-A800-P1 (May 1961).

58. _____, "Scattering af Electromagnetic Waves from Spheres and Cylinders Coated With a Dielectric Material," Westinghouse Research Laboratories, Research Report 806-A800-R2 (May 1962).

59. _____, "Scattering from a Cylinder Coated with a Dielectric Material," in Electramagnetic Theory and Antennas, E. C. Jardan, editar, 133-144, (Pergamon Press, N. Y., 1963).

60. J. Rheinstein, "Scattering of Short Pulses of Electromagnetic Waves," Proceedings of the IEEE 53, 1069-1070 (1965).

DOCUMENT CONTROL DATA - R&D

(Security classification of title, body of abstract and indexing annotation must be entered when tha overall report is classified)

1. ORIGINATING ACTIVITY *(Corporate author)*	2a. REPORT SECURITY CLASSIFICATION
Lincoln Laboratory, M. I. T.	Unclassified
	2b. GROUP
	None

3. REPORT TITLE

Backscatter from Spheres: A Short Pulse View

4. DESCRIPTIVE NOTES *(Type of report and inclusive dates)*

Technical Report

5. AUTHOR(S) *(Last name, first name, initial)*

Rheinstein, John

6. REPORT DATE	7a. TOTAL NO. OF PAGES	7b. NO. OF REFS
27 April 1966	56	61

8a. CONTRACT OR GRANT NO.	9a. ORIGINATOR'S REPORT NUMBER(S)
AF 19(628)-5167	Technical Report 414
b. PROJECT NO. 627A	
c.	9b. OTHER REPORT NO(S) *(Any other numbers that may be assigned this report)*
d.	ESD-TR-66-169

10. AVAILABILITY/LIMITATION NOTICES

Distribution of this document is unlimited.

11. SUPPLEMENTARY NOTES	12. SPONSORING MILITARY ACTIVITY
None	Air Force Systems Command, USAF

13. ABSTRACT

The backscatter from conducting and dielectric spheres, and to a lesser extent from conducting spheres with a relatively thin dielectric coating, is considered in the time domain. Utilizing rigorously computed values of the amplitude and phase of the continuous wave hackscatter, short pulses of electromagnetic waves are synthesized by Fourier series. The resultant returns are examined as a function of time, and the individual returns compared with some approximate theories.

14. KEY WORDS

short pulse scattering
backscatter of electromagnetic waves
dielectric spheres

creeping waves
conducting spheres
physical optics